NASA MEMO 4-22-59E

NASA

MEMORANDUM

PRELIMINARY ANALYSIS OF THE EFFECT OF FLOW SEPARATION DUE TO ROCKET JET PLUMING ON AIRCRAFT DYNAMIC STABILITY DURING ATMOSPHERIC EXIT

By Murray Dryer and Warren J. North

Lewis Research Center
Cleveland, Ohio

NATIONAL AERONAUTICS AND SPACE ADMINISTRATION

June 1959
Declassified May 29, 1961

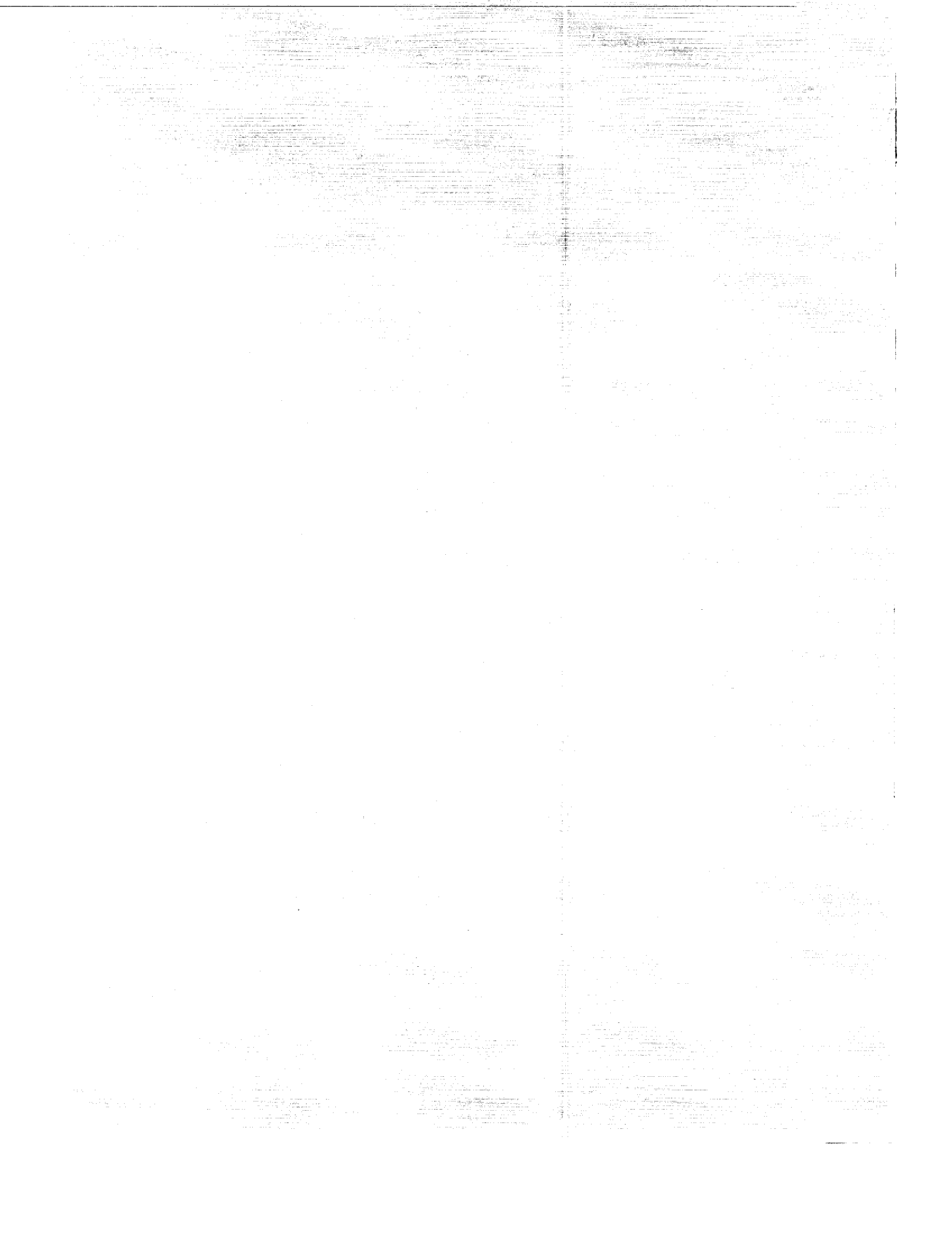

NATIONAL AERONAUTICS AND SPACE ADMINISTRATION

MEMORANDUM 4-22-59E

PRELIMINARY ANALYSIS OF THE EFFECT OF FLOW SEPARATION DUE TO ROCKET JET PLUMING ON AIRCRAFT DYNAMIC STABILITY DURING ATMOSPHERIC EXIT*

By Murray Dryer and Warren J. North

SUMMARY

A theoretical investigation was conducted to determine the effects of body boundary-layer separation resulting from a highly underexpanded jet on the dynamic stability of a typical rocket aircraft during an atmospheric exit trajectory. The particular flight condition studied on a digital computer for five degrees of freedom was at Mach 6.0 and 150,000 feet. In view of the unknown character of the separated flow field, two estimates of the pressures in the separated region were made to calculate the unbalanced forces and moments. These estimates, based on limited fundamental zero-angle-of-attack studies and observations, are believed to cover what may be the actual case.

In addition to a fixed control case, two simulated pilot control inputs were studied: rate-limited and instantaneous responses. The resulting motions with and without boundary-layer separation were compared for various initial conditions.

The lower of the assumed misalinement forces and moments led to a situation whereby a slowly damped motion could be satisfactorily controlled with rate-limited control input. The higher assumption led to larger amplitude, divergent motions when the same control rates were used. These motions were damped only when the instantaneous control responses were assumed.

INTRODUCTION

Rocket-powered aircraft have introduced several new stability and operational problems. These problems arise directly or indirectly from the high propellant flow rate, large aircraft thrust-to-weight ratio, and high combustion chamber pressure. The high flow rate, in combination

*Title, Unclassified.

with the large propellant-to-gross weight ratio, results in upstream and downstream, as well as normal and transverse, shifts in center of gravity. The importance of these center-of-gravity shifts has increased with the trend to higher thrust-to-gross weight ratios. Consequently, a great deal of attention has been given in the past to the attendant thrust vector misalinements.

Another aircraft stability problem which will become more severe at the higher altitudes is the effect of body boundary-layer separation on the fuselage due to underexpansion of the engine exhaust nozzle. From weight, size, and cooling considerations the nozzle exit area is usually designed for full expansion at some altitude considerably below the maximum which will be encountered during powered flight. Consequently, at high altitudes the underexpanded jet will plume and may induce boundary-layer separation forward on the fuselage. The higher static pressures in the separated region can cause an unbalanced force on the airplane if the separation is asymmetric. This force will create a pitching or yawing moment if it does not act through the aircraft center of gravity. When the airplane is at angle of attack or sideslip, the effects of separation become even more complex. The net result could conceivably be the departure of the aircraft from the atmosphere with an undamped, high amplitude oscillation about one or more axes. Consequently, a large - perhaps prohibitive - amount of reaction control propellant would be necessary in order to achieve a scheduled reentry or satellite attitude.

This report presents the results of a study of the destabilizing effects of the separated boundary layer. The analysis is limited in the sense that the actual character and magnitudes of the separated regions have not been determined at the Mach number and Reynolds number of this study. Consequently, several assumptions based on some fundamental experimental studies and observations were necessary. Two estimates of the pressures in the separated region were made in order to calculate unbalanced forces and moments. These two estimates were postulated in order to bracket what could actually occur. The resulting terms were included in a five degree of freedom digital computer study of an assumed airplane and subjected to various initial conditions, as well as several aerodynamic control inputs.

SYMBOLS

b	wing span, ft
C_D	drag coefficient, $\frac{D}{q_O S} = C_{D_O} + \frac{dC_D}{dC_L^2} (C_{L_\alpha})^2 \alpha^2$
C_L	lift coefficient, $\frac{\text{lift}}{q_O S}$

C_l	rolling-moment coefficient, $\frac{\text{rolling moment}}{q_0 Sb}$
C_m	pitching-moment coefficient, $\frac{\text{pitching moment about } 0.20\ \bar{c}}{q_0 S\bar{c}}$
C_{m_0}	pitching-moment coefficient at zero lift
C_n	yawing-moment coefficient, $\frac{\text{yawing moment about } 0.20\ \bar{c}}{q_0 Sb}$
C_Y	lateral-force coefficient, $\frac{\text{lateral force}}{q_0 S}$
$\bar{c}$	wing mean aerodynamic chord
D	drag
g	acceleration due to gravity at earth's surface, ft/sec^2
I_x, I_y, I_z	moments of inertia about x, y, and z body axes (assumed to be alined with principal axes), slug-sq ft
i_t	stabilizer deflection, deg
M	pitching moment about $0.20\ \bar{c}$, ft-lb
m	mass of airplane, W/g, slugs
P	static pressure
p, q, r	angular velocities about the x, y, and z body axes, rad/sec
q_0	free-stream dynamic pressure
S	wing area, sq ft
T	period, sec
t	time, sec
V	free-stream velocity, ft/sec
W	aircraft weight, lb
x, y, z	aircraft principal axes, assumed identical with body axes
x_1	moment arm of Z_{rkt} about aircraft center of gravity $(0.20\ \bar{c})$, ft

x_2 moment arm of Y_{rkt} about aircraft center of gravity $(0.20\ \bar{c})$, ft

Y_{rkt} unbalanced lateral force parallel to y axis due to rocket jet plume effect, lb

Z_{rkt} unbalanced vertical force parallel to z axis due to rocket jet plume effect, lb

α angle of attack of principal x axis, deg

β angle of sideslip, deg

δ_a, δ_v differential aileron ("rolling tail") and vertical tail deflection, respectively, deg

θ Euler pitch angle, deg

φ Euler roll angle, deg

$C_{L_{i_t}}$ $\dfrac{\partial C_L}{\partial i_t}$

C_{L_α} $\dfrac{\partial C_L}{\partial \alpha}$

C_{l_p} $\dfrac{\partial C_l}{\partial \frac{pb}{2V}}$

C_{l_r} $\dfrac{\partial C_l}{\partial \frac{rb}{2V}}$

C_{l_β} $\dfrac{\partial C_l}{\partial \beta}$

$C_{l_{\delta_a}}$ $\dfrac{\partial C_l}{\partial \delta_a}$

$C_{l_{\delta_v}}$ $\dfrac{\partial C_l}{\partial \delta_v}$

$C_{m_{i_t}}$ $\dfrac{\partial C_m}{\partial i_t}$

C_{m_q}	$\frac{\partial C_m}{\partial \frac{q\bar{c}}{2V}}$
C_{m_α}	$\frac{\partial C_m}{\partial \alpha}$
$C_{m_{\dot{\alpha}}}$	$\frac{\partial C_m}{\partial \frac{\dot{\alpha}\bar{c}}{2V}}$
$C_{m_{\beta^2}}$	$\frac{\partial C_m}{\partial \beta^2}$
C_{n_p}	$\frac{\partial C_n}{\partial \frac{pb}{2V}}$
C_{n_r}	$\frac{\partial C_n}{\partial \frac{rb}{2V}}$
C_{n_β}	$\frac{\partial C_n}{\partial \beta}$
$C_{n_{\delta_a}}$	$\frac{\partial C_n}{\partial \delta_a}$
$C_{n_{\delta_v}}$	$\frac{\partial C_n}{\partial \delta_v}$
C_{Y_r}	$\frac{\partial C_Y}{\partial \frac{rb}{2V}}$
C_{Y_β}	$\frac{\partial C_Y}{\partial \beta}$
$C_{Y_{\delta_a}}$	$\frac{\partial C_Y}{\partial \delta_a}$
$C_{Y_{\delta_v}}$	$\frac{\partial C_Y}{\partial \delta_v}$

Dot over symbol represents derivative with respect to time. Moments referred to 0.20 $\bar{c}$, body axis system.

Subscripts:

e	nozzle exit
w	wake
1	prior to separated region
2	separated region

PROCEDURE

Preliminary Considerations and Assumptions

The basic physical phenomenon involved in this discussion is the underexpanded rocket jet exhaust which will be referred to as the "jet plume." It will be assumed that the plume will leave the rocket nozzle at a very high angle with respect to the external flow as shown[1] schematically in figure 1. As noted earlier, this plume interacts with the external flow exactly as in the case of the solid surfaces, shown, for example, in references 1 to 4. The longitudinal extent and angle of the subsequent boundary-layer separation, as shown by these investigators, is a function of the Mach number and Reynolds number as well as the angle of the disturbing body (c.f., the missile afterbody flare angle in refs. 2 and 4).

With the use of these fundamental experiments as well as some unpublished observations, a first estimate of the pressure in the separated region was made using a two-dimensional separation angle of 11°. However, since the present analysis is concerned with a Mach and Reynolds number combination which has not been treated in the current literature, an extreme value of the separation deflection angle (30°) was assumed for a second and limiting calculation.[2] This value may be extreme; however, it is believed that, for the purposes of this report, any overprediction will change only the magnitudes of the results and not the

---

[1]Some justification of this high angle of initial expansion is described as follows: Calculations (ref. 5) of a typical rocket propellent-nozzle combination resulted in a jet exit static-pressure ratio of the order of 400 for the assumed altitude. As shown in reference 6, the initial expansion angle can be on the order of 80°.

[2]This value was also used as an example in reference 6 to indicate the decrease in the initial angle of the jet boundary if separation were to occur.

principles involved. As a result the ratios of pressure in the separated region (P_2) to local free-stream pressure (P_1) were 4.0 and 17.7 for the 11° and 30° assumptions, respectively. In both cases P_1 was assumed equal to free-stream static pressure.

In order to calculate the forces and corresponding moments due to the pressures mentioned above, it was necessary to assume a variation of the separated region with angle of attack. At zero angle of attack it was assumed that asymmetric separation occurred because of the fuselage asymmetry introduced by the pilot's canopy. The separation area (schematically indicated as the shaded area in figs. 1(a) and (b)) was assumed to increase linearly with angle of attack and then to remain constant for angles of attack greater than 10°. Any lateral separation at zero sideslip was assumed symmetrical and was omitted from the figure.

The resulting separation forces and moment arms are presented in figure 2 as functions of angles of attack and sideslip for the two pressure-ratio estimates. The forces and moments were added to the appropriate equations of motion for five degrees of freedom. The resulting equations, table I, were programmed into an IBM 653 digital computer and solved for a zero-lift flight trajectory in the vicinity of rocket burnout. The aircraft was assumed to be climbing at a flight path angle of 22.5° at an altitude of 150,000 feet with a flight Mach number of 6.0. A 10-second flight history was calculated assuming constant dynamic pressure and stability derivatives compatible with a Mach number of 6.0. The airplane parameters and stability derivatives are given in table II. The derivatives are appropriate for use in the absence of flow separation; however, the basic derivatives (C_{L_α}, C_{Y_β}, C_{m_α}, C_{n_β}) may be considered as being changed by the addition of the terms discussed earlier. The damping derivatives were assumed to be unaffected.

Initial Conditions and Control Input

Initial conditions included several angles of sideslip, and various pitching, yawing, and rolling-rate combinations.

The initial values of α or β influence the magnitudes of forces and moments due to the jet interference flow field that are introduced as step[3] disturbances at $t = 0$; the motions resulting therefrom will be discussed in the Rocket Engine Operating section. Rocket-engine burnout and flow reattachment were assumed to occur at $t = 3$ seconds.

---

[3]Additional runs were calculated to compare the motions resulting from ramp inputs with those from step inputs. The magnitudes of the resulting oscillations were similar.

During one set of calculations the flight motions were calculated with fixed controls. A second set of calculations (referred to herein as "rate-limited control") was made during which pilot input was assumed. It was assumed that the pilot would apply corrective aerodynamic control deflection proportional to angle of attack and sideslip and would also apply aerodynamic control deflection to damp out any angular velocities. It was further conservatively assumed that control effectiveness was not changed by the jet interference flow field. Pilot reaction time is short compared with the period of aircraft oscillation at high altitude and is, therefore, neglected. Control deflection angular rates were limited to values compatible with hydraulic-actuated controls. A third type of control input omitted the limitation on control deflection rate. This type of response will be referred to herein as "instantaneous." Table III lists the control-input equations as well as the limits of control deflection.

The results of the analysis, then, can be subdivided into three categories which depend on the initial conditions: (a) initial steady-state flight with no rolling, pitching, or yawing motions; (b) initial sideslip; and (c) several combinations of initial rates of roll, pitch, and yaw. The nonzero initial conditions were estimates of inadvertant motions or attitudes which might exist at high altitudes with high longitudinal accelerations and asymmetric separation forces. Table IV lists these various initial conditions as well as the assumed aerodynamic control and rocket-operation inputs. It should be noted that, although the initial pitching velocity is listed as zero for some of the initial conditions, a zero-lift trajectory dictates a very small negative value. Thus, $q(0) = 0$, as listed in the text, actually was equal to -0.00458 radians per second.

RESULTS AND DISCUSSION

Reference Data - Rocket Off

Results of the analysis assuming no body boundary-layer separation generally resulted in motions which were easily damped with the rate-limited controls. This condition then may be considered to be of interest only for providing reference information. For example, the resultant sideslip motion due to an initial sideslip of 4° shown in figure 3 is quickly damped with the controls. The stabilizer, aileron, and rudder-control-deflection histories are also shown. Similar easily damped responses were obtained for the other initial conditions as indicated in the summary of results shown in table IV.

Rocket Engine Operating: $P_2/P_1 = 4.0$

The calculated motions were obtained as follows for the lower of the assumed forces and moments:

$\alpha(0) = \beta(0) = p(0) = q(0) = r(0) = 0$. - A pitching moment due to the jet interference flow field of about 5000 foot pounds ($x_1 Z_{rkt}$) was assumed to occur at zero angle of attack as indicated on figure 2. Consequently, only pitching motions were initiated as shown in figure 4. Also shown are the comparative motions for stick-fixed and rate-limited control inputs. It is interesting to note (figs. 4(a) and (b)) that the undamped, stick-fixed, angle-of-attack motion was largely eliminated when rate-limited control inputs were used.

Initial sideslip. - The motions for an initial 4° angle of sideslip are summarized in table IV for the stick-fixed and rate-limited control inputs. As noted, the control inputs damped the motions which occurred with stick-fixed controls. Comparison of the results using control input with the "rocket-off" situation indicates that angle of attack excursions on the order of $\pm 4^\circ$ were caused by the assumed forces arising from boundary-layer separation.

Initial rates of roll, pitch, and yaw. - The motions for an initial rate of yaw, $r = 0.1$ radian per second, are also listed in table IV for stick-fixed and rate-limited control inputs. Use of the rudder prior to burnout decreased the maximum value of sideslip from 15° to about 2°. Calculations showed that the rate-limited control input again effectively damped the motions in sideslip and roll after burnout. Similar results (table IV) were obtained with simultaneous initial rates of pitch and yaw.

Results for simultaneous initial rates of roll, pitch, and yaw (0.1 rad/sec in each case) are shown in figure 5. It is of interest to note (fig. 5(a)) that the slope of the pitch rate changed discontinuously at burnout. The removal of the smaller lateral force (Y_{rkt}) at burnout caused a negligible change in the yaw-rate slope.

Rocket Engine Operating; $P_2/P_1 = 17.7$

The calculated motions for the higher of the two assumed forces arising from boundary-layer separation will now be discussed. Instantaneous corrective control input was assumed in addition to the previously considered stick-fixed and rate-limited control input.

$\alpha(0) = \beta(0) = p(0) = q(0) = r(0) = 0$. - The motions resulting from stick-fixed and rate-limited control input are shown in figures 6(a) and (b). It can be seen that the high positive angle of attack of about 33° prior to burnout was decreased to 29° by the incorporation of horizontal stabilizer control, and the amplitudes of the pitching oscillations were reduced. Again, a discontinuous change occurred in the slope of the pitching rate at burnout. When instantaneous control was considered (shown in fig. 6(c)) the angle-of-attack oscillations were quickly damped

after burnout. Prior to burnout, however, the horizontal stabilizer was unable to decrease the 29°-angle-of-attack excursion.

Initial sideslip. - The response for an initial 4° angle of sideslip is shown in figure 7(a) for the stick-fixed condition. The large undamped sideslip oscillation between 0° and 43° is immediately apparent. The angle-of-attack oscillation, although large, was slowly damped. However, the aerodynamic coupling caused a roll rate at $t = 2$ seconds of about 1.0 radian per second which remained fairly constant for at least the remainder of the 10-second test period.

Figure 7(b) shows the response when rate-limited controls were used. The roll condition was damped very satisfactorily due to aileron (or "rolling tail") and rudder control. The sideslip oscillation, however, was not improved. Furthermore, the angle of attack reached a maximum negative value at 5.2 seconds of about -26° with a slowly (about 4-sec period) diverging oscillation in spite of horizontal stabilizer control. This angle-of-attack divergence was eliminated by the instantaneous control input as shown in figure 7(c). The sideslip and roll motions were also satisfactorily controlled, although the large sideslip angle of about 30° was unavoidable prior to burnout.

The response for the smaller initial angles of sideslip were similar in nature to those described, except as follows: the magnitudes of the maximum negative angle-of-attack excursions were smaller; the maximum positive angles of attack, however, remained about the same as those just mentioned. In all cases, an abrupt slope change in the pitching rate occurred at burnout.

Initial rates of roll, pitch, and yaw. - When an initial yaw rate of -0.1 radian per second was assumed, the response was very similar to that described for the initial sideslip condition. Also, as shown in figure 8, similar results were obtained with $r(0) = +0.1$ radian per second. In fact, the salient features of the response were unchanged when additional initial conditions, $p(0) = q(0) = +0.1$ radian per second, were added as indicated in table IV. Maximum normal accelerations were on the order of 2 g's which are within structural and human tolerance levels. These accelerations, calculated at the maximum positive angles of attack, also considered the simultaneous maximum negative pitching acceleration.

CONCLUDING REMARKS

The effects of rocket-engine operation and burnout on the dynamic stability of a rocket airplane at Mach 6.0 and 150,000 feet have been theoretically examined in some detail for several initial conditions. The present analysis is limited in the sense that the actual character

and magnitudes of the separated regions with the associated forces are unknown. As a result they had to be postulated on the basis of limited fundamental zero-angle-of-attack separation studies (refs. 1, 2, and 3). Accordingly, boundary-layer separation patterns were assumed as a function of angle of attack and sideslip. Corresponding separation force and moment inputs were calculated on the basis of two assumed pressure ratios across separation-induced oblique shocks. In addition, several aerodynamic control inputs (stick-fixed, rate-limited, and instantaneous response) were studied. Aerodynamic control effectiveness was considered to be unaffected by the jet interference flow field for the rate-limited and instantaneous inputs.

The results for the lower pressure-ratio assumption indicate, for stick-fixed controls, slowly damped angle of attack and sideslip motions. The rate-limited control input resulted in quick damping of these motions. The results for the higher pressure-ratio assumption, considered to be a limiting situation, produced large stick-fixed oscillations. The rate-limited control response caused the oscillations to become divergent in some cases. When instantaneous control response was utilized, the instability was eliminated.

Should separation occur, then, the situation at best appeared to be within pilot controllability. If the extreme separation pressure ratio were considered, fast control responses would be necessary to reduce oscillatory and rolling motions to manageable values.

Lewis Research Center
National Aeronautics and Space Administration
Cleveland, Ohio, January 27, 1959

REFERENCES

1. Chapman, Dean R., Kuehn, Donald M., and Larson, Howard K.: Investigation of Separated Flows in Supersonic and Subsonic Streams with Emphasis on the Effect of Transition. NACA TN 3869, 1957.

2. Dennis, David H.: The Effects of Boundary-Layer Separation over Bodies of Revolution with Conical Tail Flares. NACA RM A57I30, 1957.

3. Moeckel, W. E.: Flow Separation Ahead of a Blunt Axially Symmetric Body at Mach Number 1.76 to 2.10. NACA RM E51I25, 1951.

4. Becker, John V., and Korycinski, Peter F.: Heat Transfer and Pressure Distribution at a Mach Number of 6.8 on Bodies with Conical Flares and Extensive Flow Separation. NACA RM L56F22, 1956.

5. Gordon, Sanford, and Glueck, Alan R.: Theoretical Performance of Liquid Ammonia with Liquid Oxygen as a Rocket Propellant. NACA RM E58A21, 1958.

6. Love, Eugene S., and Lee, Louise P.: Shape of Initial Portion of Supersonic Axisymmetric Free Jets at Large Jet Pressure Ratios. NACA TN 4195, 1958.

TABLE I. - EQUATIONS OF MOTION AND EULERIAN ANGULAR VELOCITIES

[Principal axes system.]

Equations of motion:

$$\dot{\alpha} = q - p\frac{\sin\beta}{\cos\alpha\cos\beta} + \frac{g}{V}\frac{\cos\theta\cos\varphi}{\cos\alpha\cos\beta} - \frac{q_0 S}{mV\cos\beta}C_{L_\alpha}\alpha - \frac{q_0 S}{mV\cos\beta}C_{L_{i_t}}i_t - \frac{q_0 S}{mV\cos\beta}C_D\frac{\sin\alpha}{\cos\alpha} + \frac{Z_{rkt}}{mV\cos\alpha\cos\beta}$$

$$\dot{\beta} = p\sin\alpha - r\cos\alpha + \frac{g}{V}\frac{\sin\varphi\cos\theta}{\cos\beta} + \frac{q_0 S}{mV}\frac{C_{Y_\beta}\beta}{\cos\beta} + \frac{q_0 Sb}{2mV^2}C_{Y_r}\frac{r}{\cos\beta} + \frac{q_0 S}{mV\cos\beta}C_{Y_{\delta_a}}\delta_a + \frac{q_0 S}{mV\cos\beta}C_{Y_{\delta_v}}\delta_v + \frac{Y_{rkt}}{mV\cos\beta}$$

$$\dot{p} = \frac{I_y - I_z}{I_x}qr + \frac{q_0 Sb}{I_x}C_{l_{\delta_a}}\delta_a + \frac{q_0 Sb^2}{2VI_x}C_{l_p}p + \frac{q_0 Sb^2}{2VI_x}C_{l_r}r + \frac{q_0 Sb}{I_x}C_{l_\beta}\beta + \frac{q_0 Sb}{I_x}C_{l_{\delta_v}}\delta_v$$

$$\dot{q} = \frac{I_z - I_x}{I_y}pr + \frac{q_0 S\bar{c}}{I_y}C_{m_\alpha}\alpha + \frac{q_0 S\bar{c}}{I_y}C_{m_{i_t}}i_t + \frac{q_0 S\bar{c}^2}{2VI_y}C_{m_q}q + \frac{q_0 S\bar{c}^2}{2VI_y}C_{m_{\dot{\alpha}}}\dot{\alpha} + \frac{q_0 S\bar{c}C_{m_0}}{I_y} + \frac{q_0 S\bar{c}}{I_y}C_{m_{\beta^2}}\beta^2 + \frac{Z_{rkt}x_1}{I_y}$$

$$\dot{r} = \frac{I_x - I_y}{I_z}pq + \frac{q_0 Sb}{I_z}C_{n_\beta}\beta + \frac{q_0 Sb^2}{2VI_z}C_{n_r}r + \frac{q_0 Sb^2}{2VI_z}C_{n_p}p + \frac{q_0 Sb}{I_z}C_{n_{\delta_a}}\delta_a + \frac{q_0 Sb}{I_z}C_{n_{\delta_v}}\delta_v - \frac{Y_{rkt}x_2}{I_z}$$

Eulerian angular velocities:

$$\dot{\varphi} = p + q\tan\theta\sin\varphi + r\cos\varphi\tan\theta$$

$$\dot{\theta} = q\cos\varphi - r\sin\varphi$$

TABLE II. - AIRCRAFT CONSTANTS AND STABILITY DERIVATIVES

Aircraft constants:

S, sq ft	200
m, slugs	417
b, ft	22.36
$\bar{c}$, ft	10.28
I_x, slug-sq ft	3,348
I_y, slug-sq ft	77,233
I_z, slug-sq ft	78,691

Stability derivatives (Mach number, 6.0. No jet interference flow field effects.):

$$C_{L_\alpha} = \begin{cases} 0.020 + 0.0005\,\alpha; \text{ positive } \alpha \\ 0.020 - 0.0004\,\alpha; \text{ negative } \alpha \end{cases} \text{ per deg}$$

$$C_{m_\alpha} = \begin{cases} -0.000976\,\alpha; \text{ positive } \alpha \\ +0.000730\,\alpha; \text{ negative } \alpha \end{cases} \text{ per deg}$$

$$C_{m_0} = -0.010$$

$$C_D = \begin{cases} 0.0388 + 0.0003456\,\alpha^2 + 0.00001728\,\alpha^3 + 0.000000216\,\alpha^4; \text{ positive } \alpha \\ 0.0388 + 0.0003456\,\alpha^2 - 0.00001382\,\alpha^3 + 0.000000138\,\alpha^4; \text{ negative } \alpha \end{cases}$$

$$C_{L_{1_t}} = \begin{cases} 0.0026 + 0.0000112\,\alpha^2; \text{ positive } \alpha \\ 0.0025; \text{ negative } \alpha \end{cases} \text{ per deg}$$

$$C_{m_{1_t}} = \begin{cases} -0.0040 - 0.0000230\,\alpha^2; \text{ positive } \alpha \\ -0.0040; \text{ negative } \alpha \end{cases} \text{ per deg}$$

$$C_{m_{\beta^2}} = 0$$

$$C_{n_\beta} = 0.00245 + 0.0000062\,\alpha^2, \text{ per deg}$$

$$C_{l_\beta} = \begin{cases} -0.00004 - 0.0000235\,\alpha; & -7.6^\circ < \alpha < 9.4^\circ \\ -0.00067 + 0.000049\,\alpha; & \alpha > 9.4^\circ \\ +0.00025 + 0.00002\,\alpha; & \alpha < -7.6^\circ \end{cases} \text{ per deg}$$

$$C_{y_\beta} = -0.0159 - 0.0000188\,\alpha, \text{ per deg}$$

$$C_{m_q} = -3.25 - 0.095\,\alpha, \text{ per rad}$$

$$C_{m_{\dot{\alpha}}} = 0$$

$$C_{n_p} = -0.18 \sin 7.2\,\alpha, \text{ per rad}$$

$$C_{n_r} = -0.68 - 0.00105\,\alpha^2, \text{ per rad}$$

$$C_{l_p} = -0.14 \cos 3\alpha, \text{ per rad}$$

$$C_{l_r} = 0.15\,|\sin 9\alpha|, \text{ per rad}$$

$$C_{n_{\delta_v}} = -0.0025, \text{ per deg}$$

$$C_{l_{\delta_v}} = 0.00015 - 0.00004\,\alpha, \text{ per deg}$$

$$C_{y_{\delta_v}} = 0.0040, \text{ per deg}$$

$$C_{l_{\delta_a}} = 0.00020 + 0.0000007\,(\alpha + 16)^2, \text{ per deg}$$

$$C_{n_{\delta_a}} = 0.00025 + 0.0000075\,\alpha, \text{ per deg}$$

$$C_{y_{\delta_a}} = -0.0003 - 0.000013\,\alpha, \text{ per deg}$$

$$C_{y_r} = 0$$

TABLE III. - CONTROL INPUT EQUATIONS

Rated-limited input:

$i_t = 3\alpha + 75\dot{\alpha}$; $(\dot{i}_t)_{max} = 15^\circ/sec$

$\delta_v = -1.5\ \beta - 75\dot{\beta}$; $(\dot{\delta}_v)_{max} = 10^\circ/sec$

$\delta_a = -1.0\ \varphi - 75\dot{\varphi}$; $(\dot{\delta}_a)_{max} = 30^\circ/sec$

Instantaneous input:

$i_t = 3\alpha + 75\dot{\alpha}$

$\delta_v = -1.5\ \beta - 75\dot{\beta}$

$\delta_a = -1.0\ \varphi - 75\dot{\varphi}$

Control limits:

$-35^\circ \leq i_t \leq 15^\circ$

$-7.5^\circ \leq \delta_v \leq 7.5^\circ$

$-15^\circ \leq \delta_a \leq 15^\circ$

TABLE IV. - SUMMARY OF RESULTS
$[0 \leq t \leq 10]$

Initial conditions					Rocket Operation ($0 \leq t < 3$)					
					Off	$P_2/P_1 = 4.0$		$P_2/P_1 = 17.7$		
					Control input					
α	β	p	q	r	Rate-limited	Stick-fixed	Rate-limited	Stick-fixed	Rate-limited	Instantaneous
0	0	0	0	0	No response	Fig. 4(a) $-16 < \alpha < 14$ (T = 5.6; critical)	Fig. 4(b) $-4 < \alpha < 5$ (T = 4.8; damped)	Fig. 5(a) $-24 < \alpha < 33$ (T = 4.9; critical)	Fig. 6(b) $-11 < \alpha < 29$ (T = 4.9; divergent)	Fig. 6(c) $-4 < \alpha < 29$ (Damped)
0	1°	0	0	0	$\Delta\alpha \approx 0$ $-1 < \beta < 1$ (Damped)	$-16 < \alpha < 14$ (T = 5.6; critical) $-5 < \beta < 3$ φ increasing	$-3 < \alpha < 5$ (T = 5.0 damped) $0 < \beta < 1$ $\varphi = 0$	$-22 < \alpha < 32$ (T = 3.2; critical) $-2 < \beta < 35$ (T = 3.1) φ increasing	$-5 < \alpha < 29$ (Damped) $-18 < \beta < 22$ (T = 6.5) $\varphi = 0$	$-5 < \alpha < 29$ (Damped) $-12 < \beta < 22$ (T = 6.2) $\varphi = 0$
0	-5°	0	0	0	$\Delta\alpha \approx 0$ $-1 < \beta < 2$ (Damped)	$-12 < \alpha < 14$ (T = 5.7; critical) $-8 < \beta < 4$ φ increasing	$-4 < \alpha < 5$ (T = 4.8; damped) $0 < \beta < 2$ $\varphi = 0$	$-22 < \alpha < 30$ (T = 3.0) $2 < \beta < 40$ φ increasing	$-23 < \alpha < 27$ (Divergent) $-15 < \beta < 25$ $\varphi = 0$	$-8 < \alpha < 27$ (Damped) $-13 < \beta < 24$ $\varphi = 0$
0	4°	0	0	0	Fig. 3 $\Delta\alpha \approx 0$ $-1 < \beta < 4$ (Damped)	$-17 < \alpha < 14$ (T = 5.6) $-10 < \beta < 6$ φ increasing	$-4 < \alpha < 5$ (T = 4.8; damped) $-1 < \beta < 4$ $\varphi = 0$	Fig. 7(a) $-29 < \alpha < 31$ (T = 3.0) $0 < \beta < 43$ φ increasing	Fig. 7(b) $-28 < \alpha < 26$ (Divergent) $-12 < \beta < 25$ $\varphi = 0$	Fig. 7(c) $-12 < \alpha < 26$ (Damped) $-11 < \beta < 29$ $\varphi = 0$
0	0	0	0	-0.1	$\Delta\alpha \approx 0$ $-1 < \beta < 4$ (Damped	$-20 < \alpha < 16$ (T = 5.2) $-14 < \beta < 12$ φ increasing	$-4 < \alpha < 5$ (T = 4.6) $-2 < \beta < 7$ $\varphi = 0$	$-35 < \alpha < 36$ (Divergent $-29 < \beta < 44$ φ increasing	$-30 < \alpha < 36$ (Divergent) $-13 < \beta < 26$ $\varphi = 0$	$-13 < \alpha < 26$ (Damped) $-12 < \beta < 30$ $-20 < \varphi < 20$
0	0	0	0	0.1	$\Delta\alpha \sim 0$ $-4 < \beta < 2$ (Damped)	$-20 < \alpha < 16$ (T = 5.1) $-12 < \beta < 15$ $0 < \varphi < 90$	$-4 < \alpha < 5$ (T = 4.6) $-7 < \beta < 2$ $\varphi = 0$	Fig. 8(a) $-37 < \alpha < 36$ (Divergent) $-45 < \beta < 30$ φ increasing	Fig. 8(b) $-29 < \alpha < 26$ (Critical) $-33 < \beta < 14$ $\varphi = 0$	Fig. 8(c) $-13 < \alpha < 26$ (Damped) $-30 < \beta < 13$ $\varphi = 0$
0	0	0	0.1	0.1	$-3 < \alpha < 4$ (T = 5.3; damped) $-5 < \beta < 2$ (Damped)	$-16 < \alpha < 16$ (T = 6.6) $-10 < \beta < 14$ (T = 11.4) $0 < \varphi < 60$	$-6 < \alpha < 9$ (T = 5.3; damped) $-6 < \beta < 2$ $\varphi = 0$	$-30 < \alpha < 30$ (T = 3.1) $-41 < \beta < 8$ φ increasing	$-26 < \alpha < 27$ (T = 4.1; critical) $-29 < \beta < 14$ $-10 < \varphi < 10$	$-11 < \alpha < 27$ (Damped) $-26 < \beta < 13$ $\varphi = 0$
0	0	-0.1	0.1	-0.1	$-3 < \alpha < 4$ (T = 5.0; damped) $-5 < \beta < 1$ (Damped)	Fig. 5(a) $-15 < \alpha < 17$ $-9 < \beta < 19$ $0 < \varphi < 100$	Fig. 5(b) $-6 < \alpha < 10$ (T = 5.6; damped) $-6 < \beta < 2$ $\varphi = 0$	$-24 < \alpha < 32$ (T = 3.2) $-37 < \beta < 20$ φ increasing	$-26 < \alpha < 28$ (T = 4.1; critical) $-28 < \beta < 15$ $-5 < \varphi < 5$	$-12 < \alpha < 27$ (Damped) $-27 < \beta < 12$ $\varphi = 0$

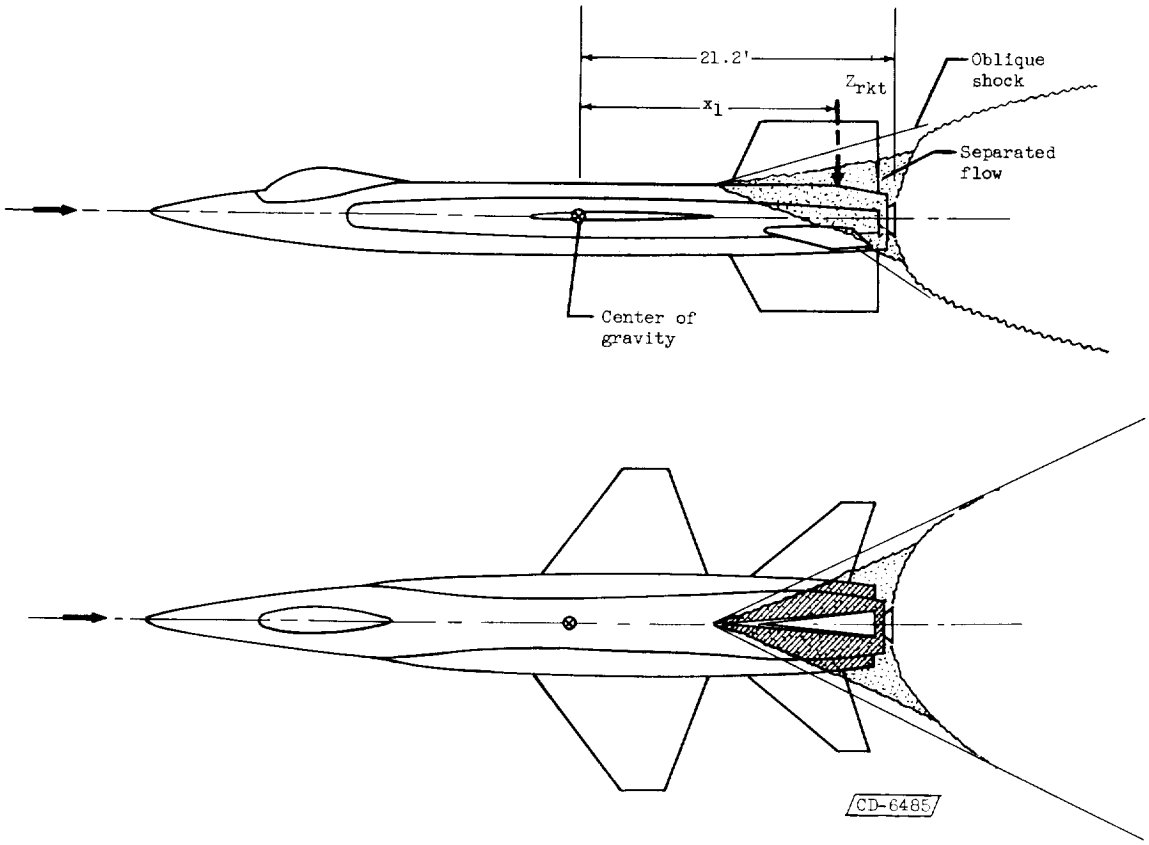

(a) Angle of attack and angle of sideslip, 0. (Note: x_l is measured from center of gravity to approximate centroid of shaded area shown in the planform view.)

Figure 1. - Assumed jet-plume-induced separation pattern. Mach number, 6.0. The shaded area in planform view indicates the projected area used for the calculation of Z_{rkt}; similar technique used in calculation of Y_{rkt}.

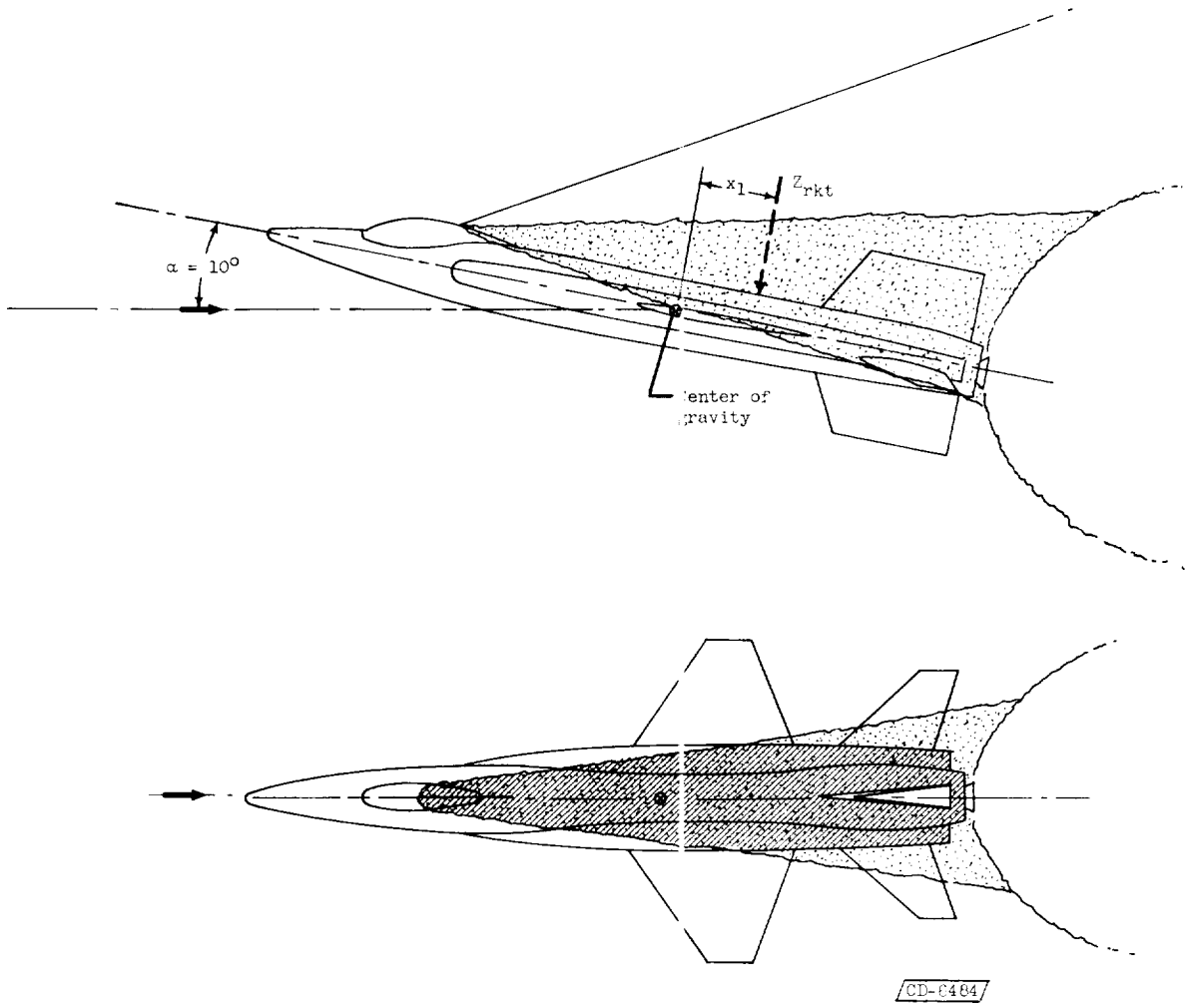

(b) Angle of attack, 10^o; angle of sideslip, 0^o.

Figure 1. - Concluded. Assumed jet-plume-induced separation pattern. Mach number, 6.0. The shaded area in planform view indicates the projected area used for calculation of Z_{rkt}; similar technique used in calculation of Y_{rkt}.

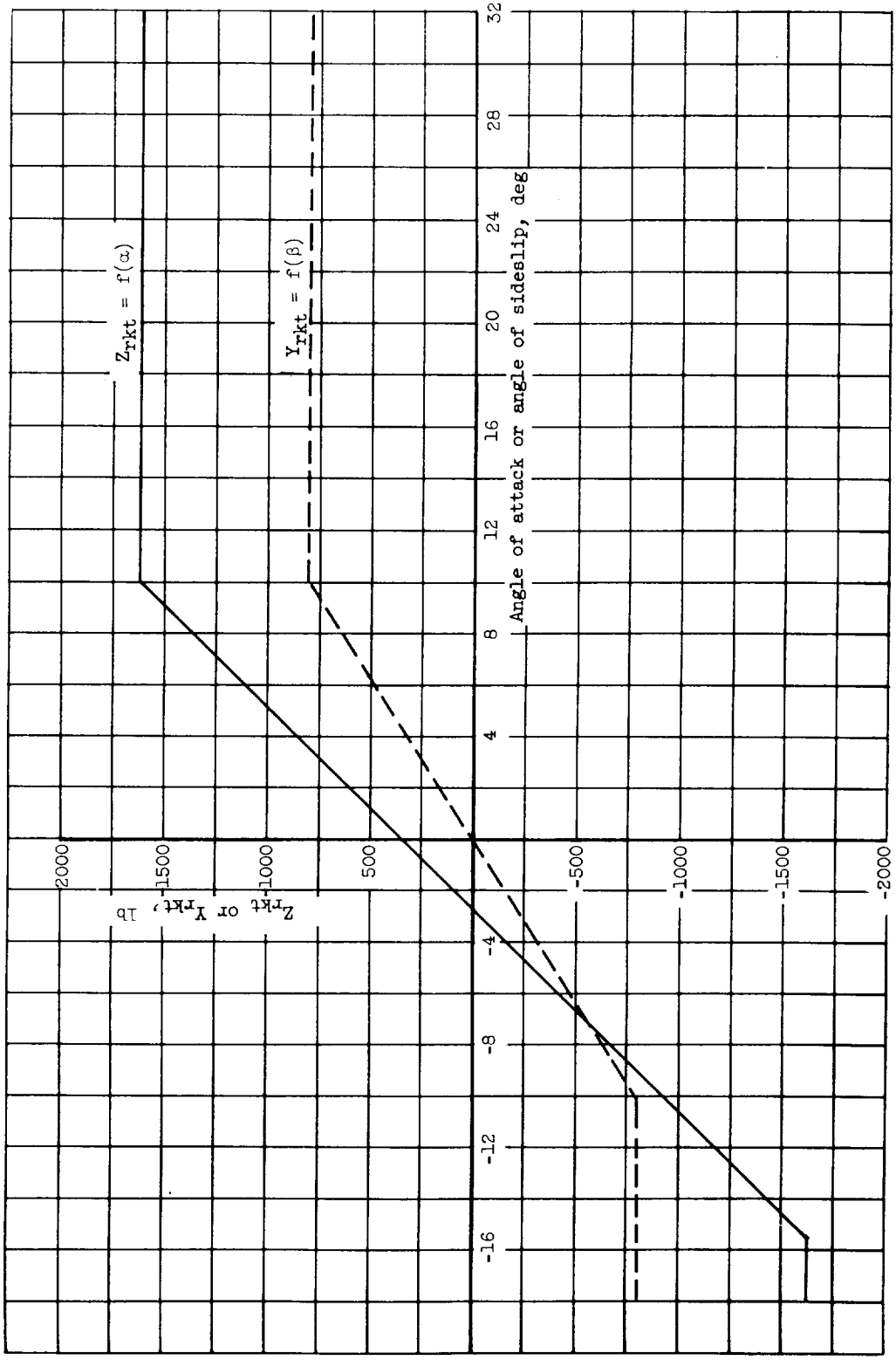

(a) Separation forces for static-pressure ratio of 4.0.

Figure 2. - Assumed separation forces (vertical and lateral) and moment arms caused by jet-plume-induced boundary-layer separation; Mach number, 6.0; altitude, 150,000 feet.

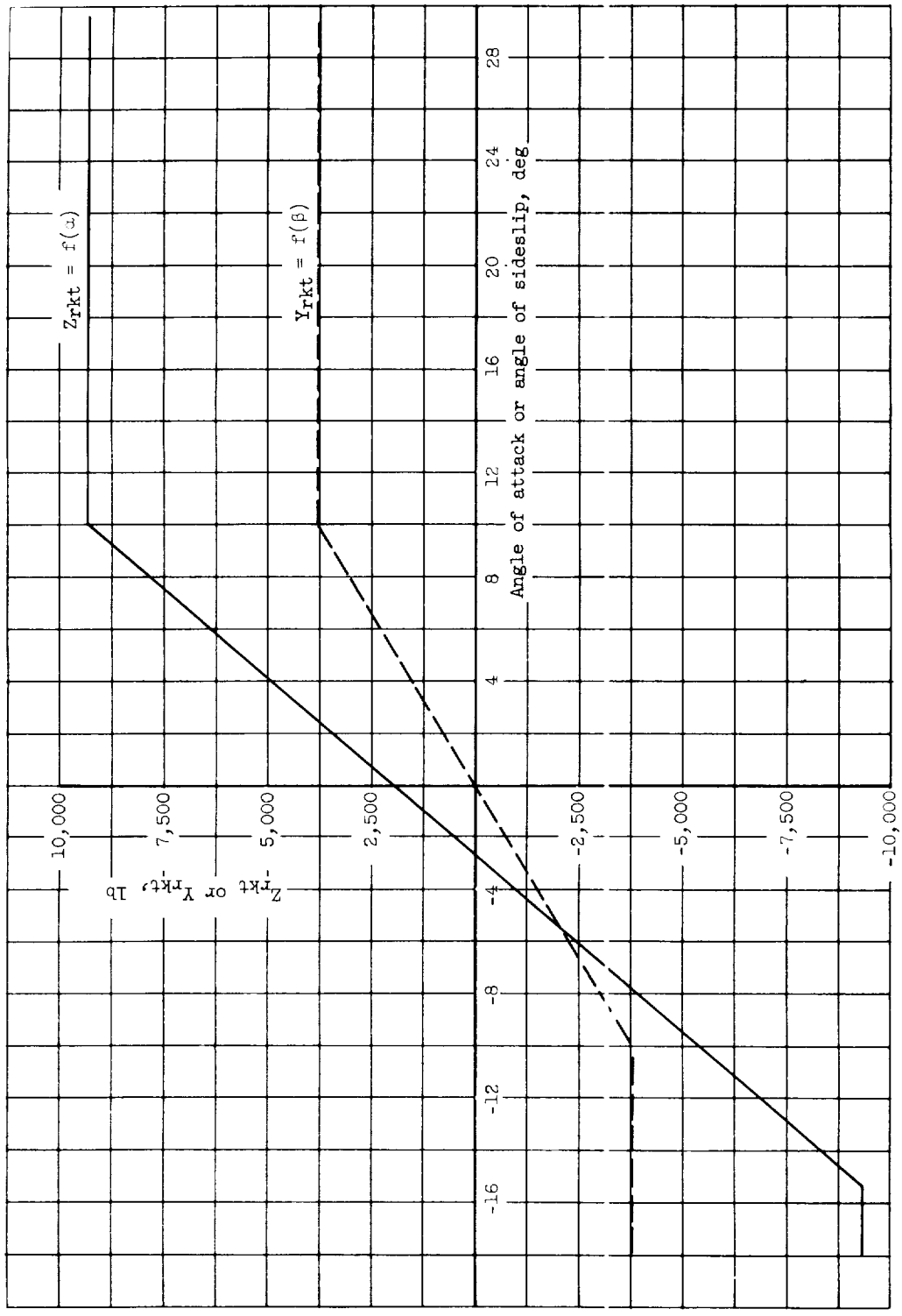

(b) Separation forces for static-pressure ratio of 17.7.

Figure 2. - Continued. Assumed separation forces (vertical and lateral) and moment arms caused by jet-plume-induced boundary-layer separation; Mach number, 6.0; altitude, 150,000 feet.

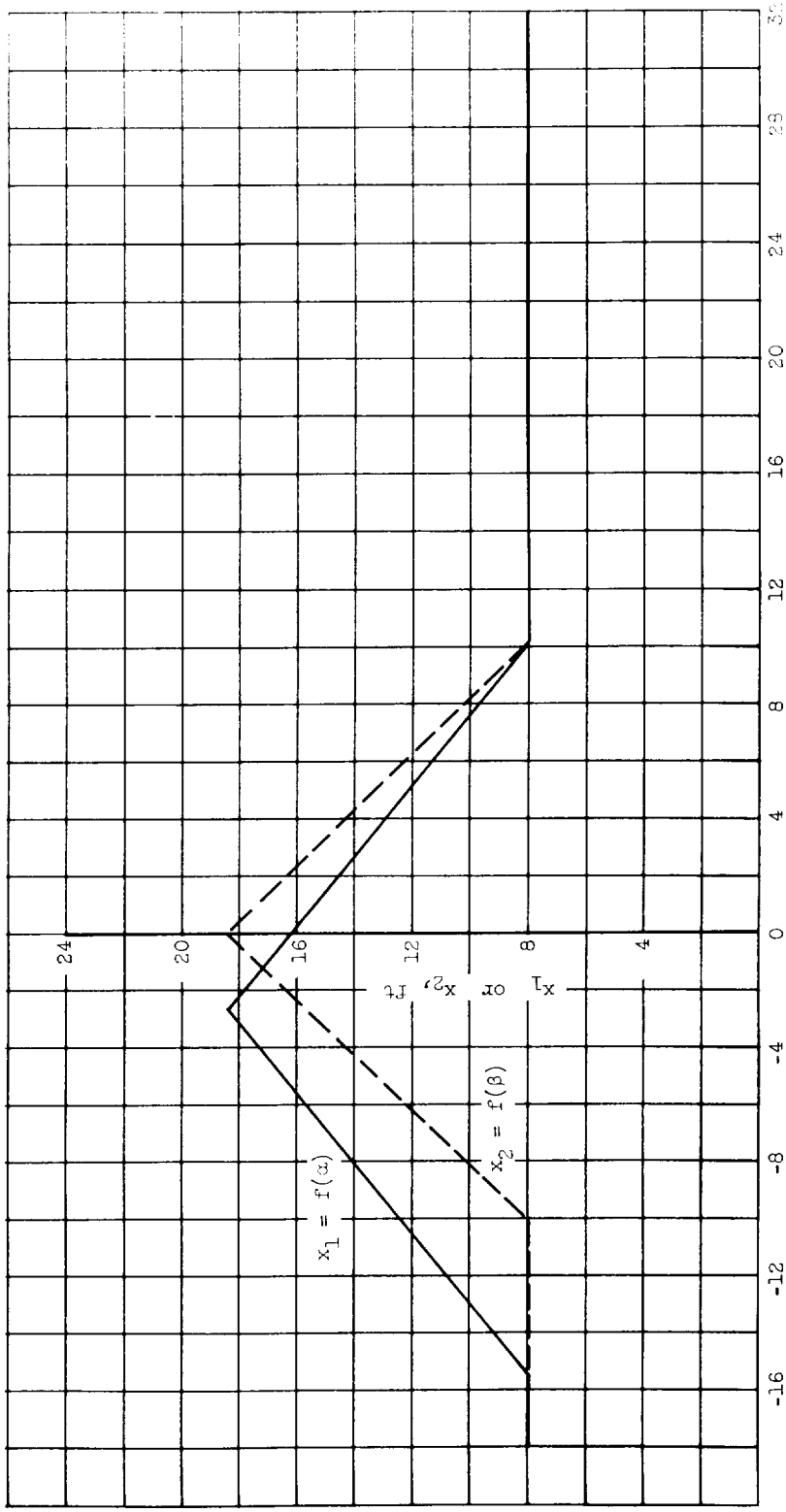

(c) Moment arms for static-pressure ratios of 4.0 and 17.7.

Figure 2. - Concluded. Assumed separation forces (vertical and lateral) and moment arms caused by jet-plume-induced boundary-layer separation; Mach number, 6.0; altitude, 150,000 feet.

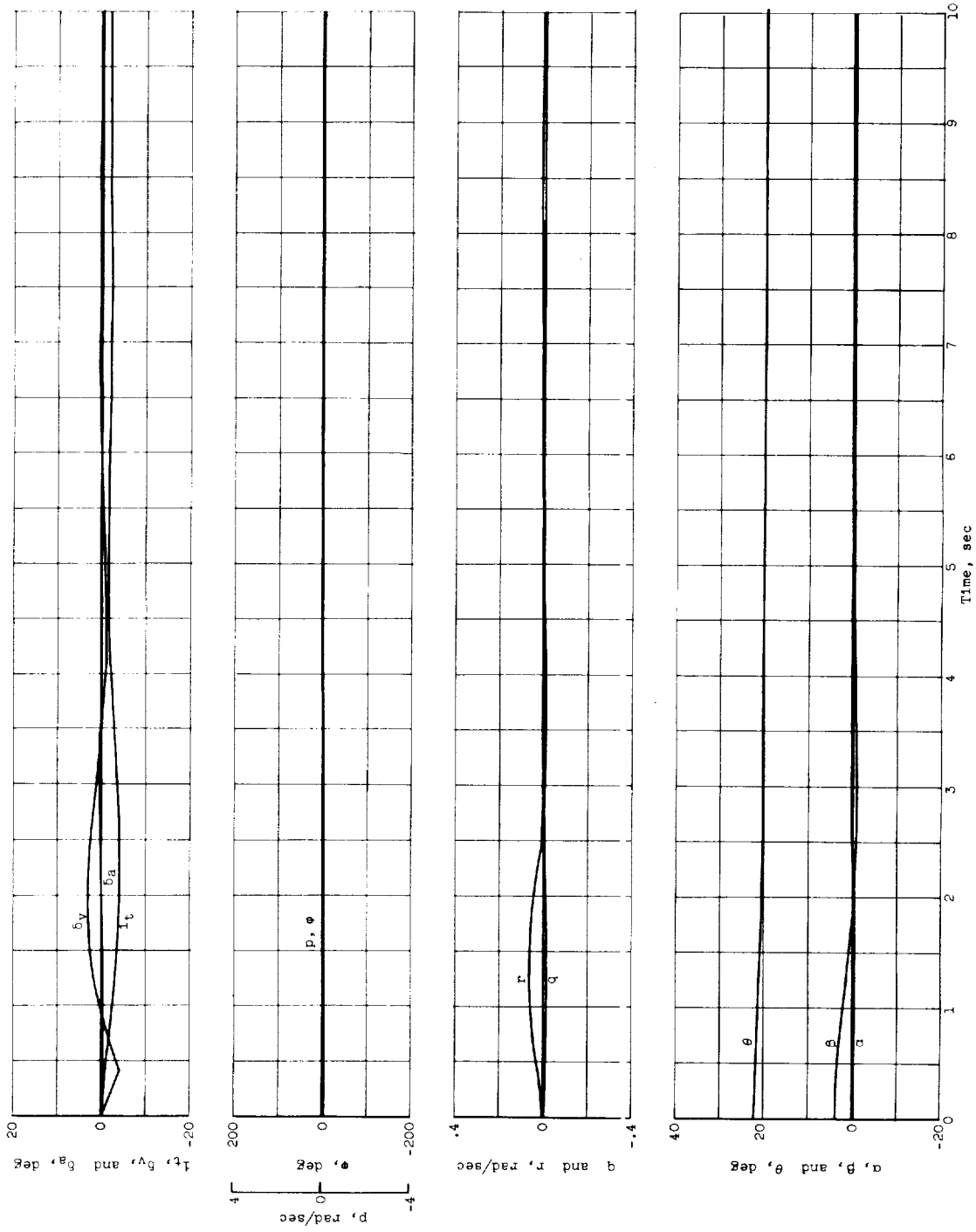

Figure 3. - Motions resulting from an initial angle of sideslip. No jet plume effect. $\beta(0) = 4^{\circ}$. Rate-limited control response.

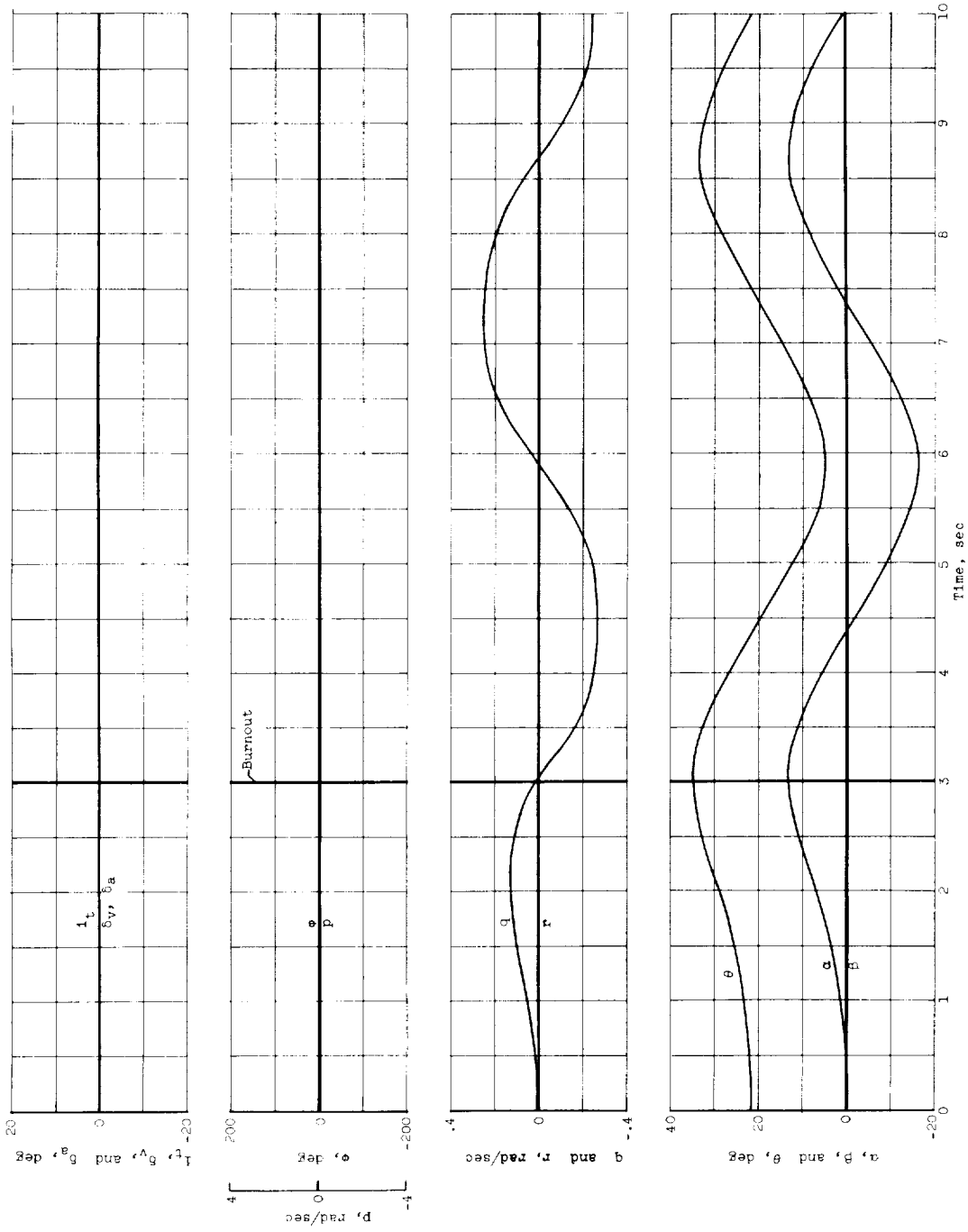

(a) Stick-fixed response.

Figure 4. - The jet plume effect ($P_2/P_1 = 4.0$) on the motions with the initial conditions: $\alpha(0) = \beta(0) = p(0) = q(0) = r(0) = 0$.

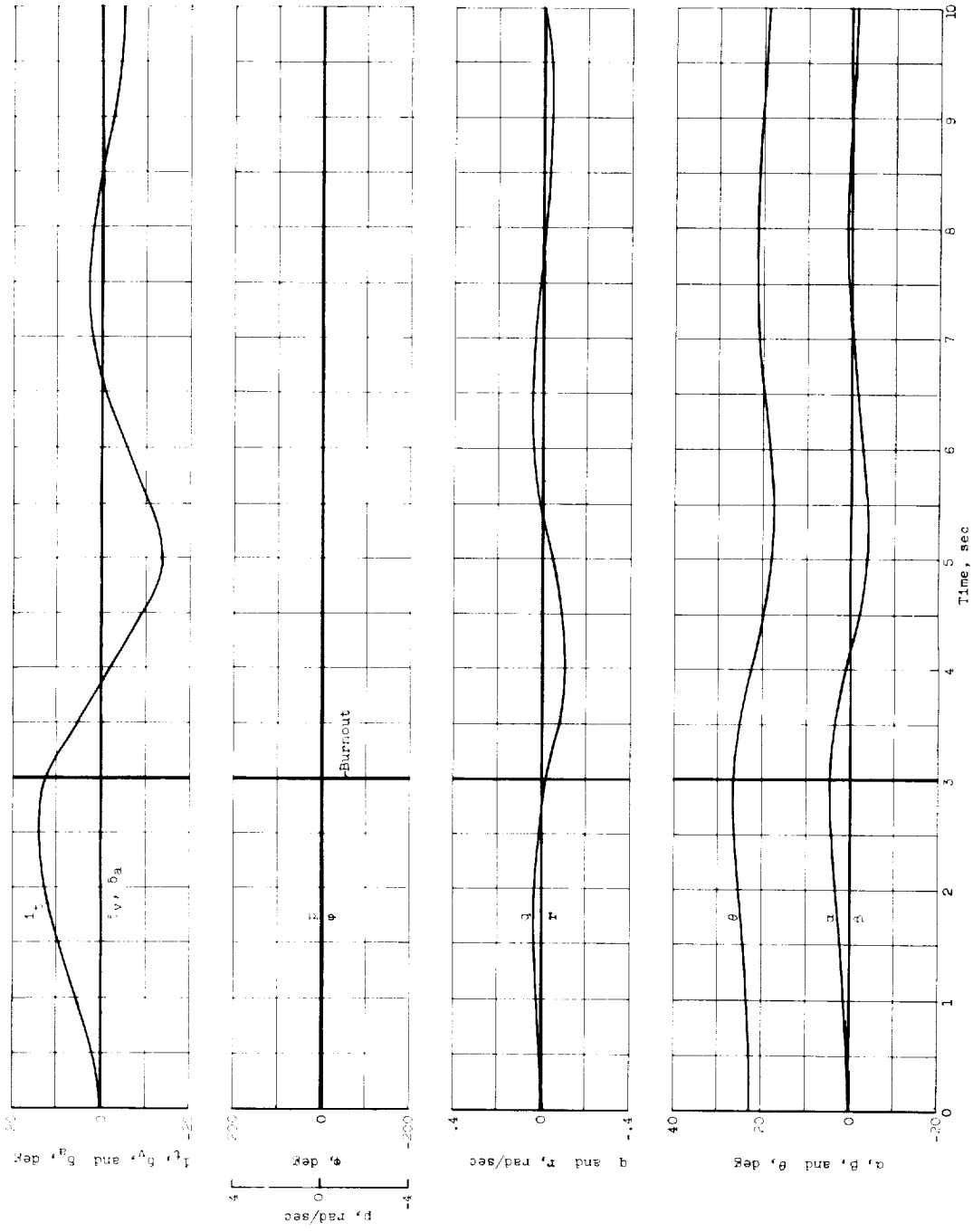

(b) Rate-limited control response.

Figure 4. - Concluded. The jet plume effect ($P_2/P_1 = 4.0$) on the motions with the initial conditions: $\alpha(0) = \beta(0) = p(0) = q(0) = r(0) = 0$.

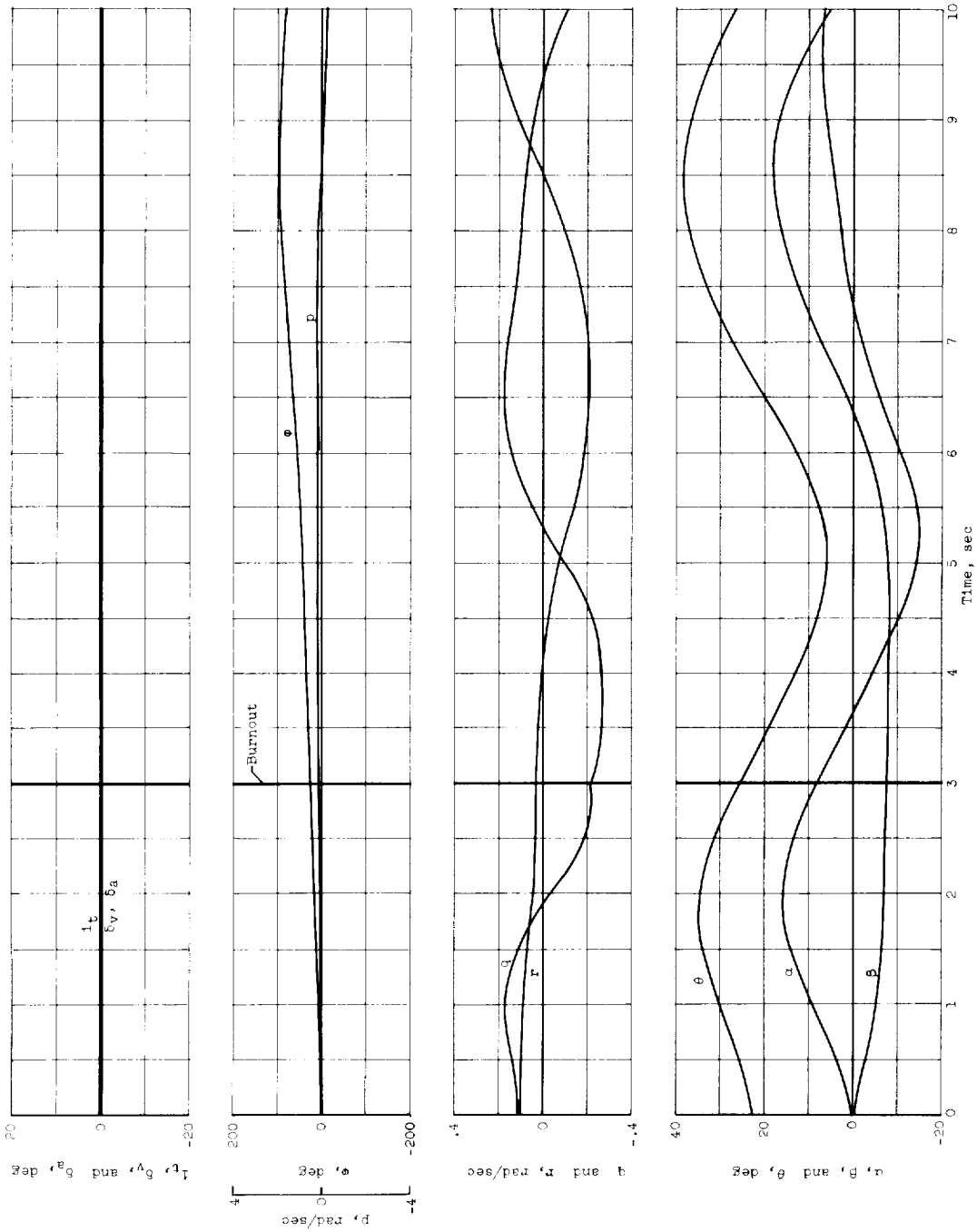

(a) Stick-fixed response.

Figure 5. - Jet plume effect ($P_2/P_1 = 4.0$) on the motions with the initial conditions: $p(0) = q(0) = r(0) = 0.1$.

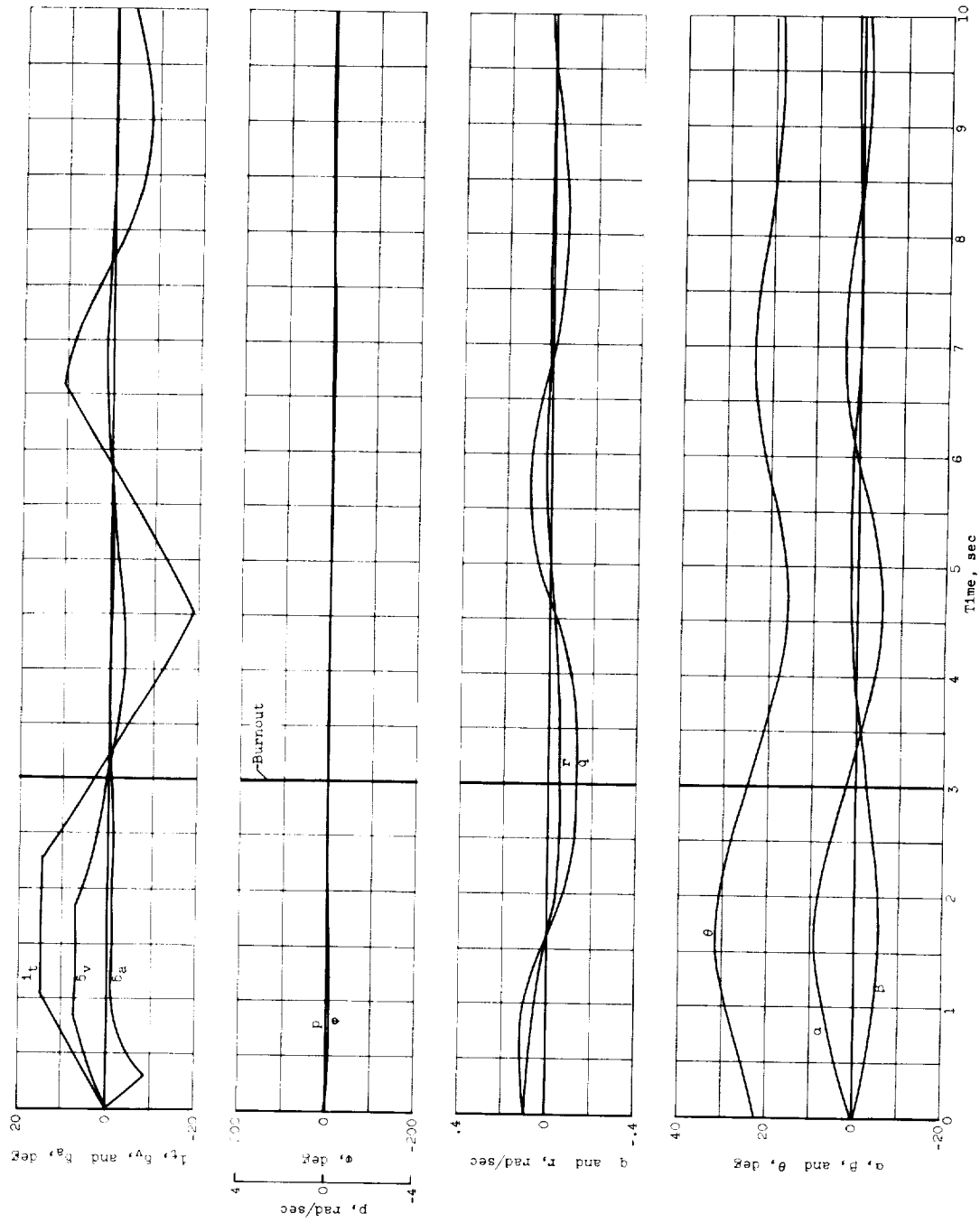

(b) Rate-limited control response.

Figure 5. - Concluded. Jet plume effect (P_2/P_1 = 4.0) on the motions with the initial conditions: p(0) = q(0) = r(0) = 0.1.

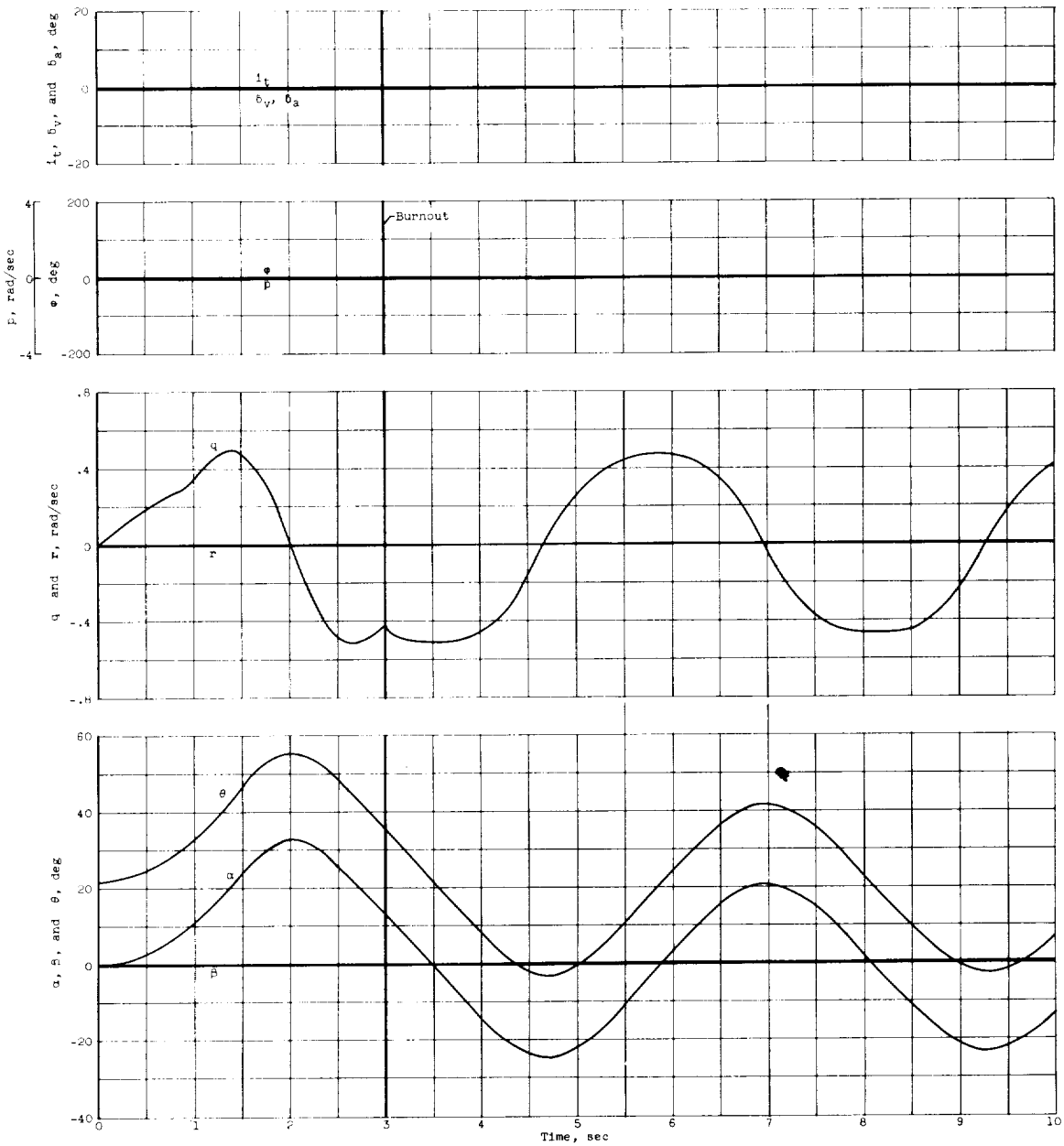

(a) Stick-fixed response.

Figure 6. - Jet plume effect (P_2/P_1 = 17.7) on the motions with the initial conditions: $\alpha(0) = \beta(0) = p(0) = q(0) = r(0) = 0$.

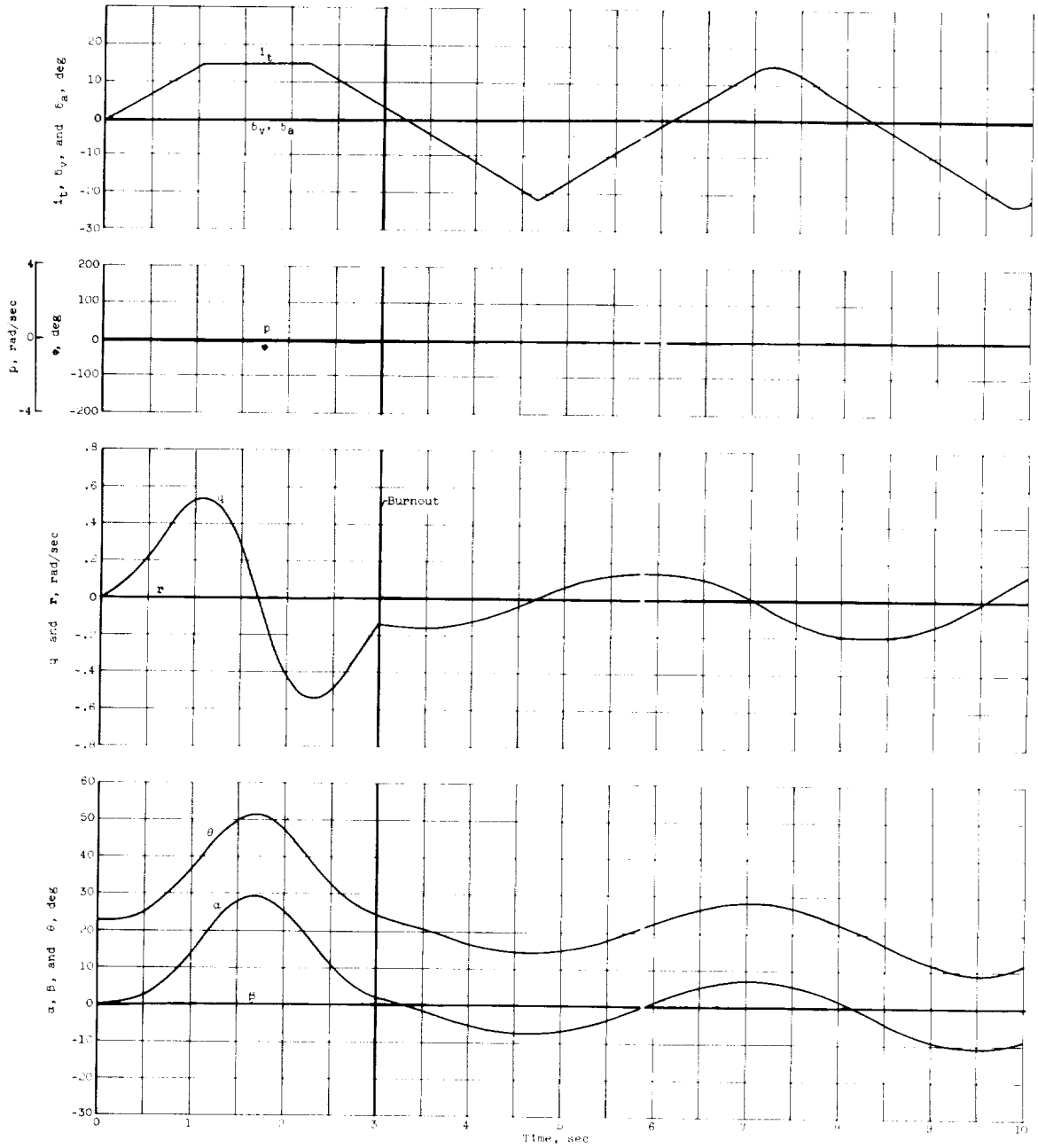

(b) Rate-limited control response.

Figure 6. - Continued. Jet plume effect (P_2/P_1 = 17.7) on the motions with the initial conditions: $\alpha(0) = \beta(0) = p(0) = q(0) = r(0) = 0$.

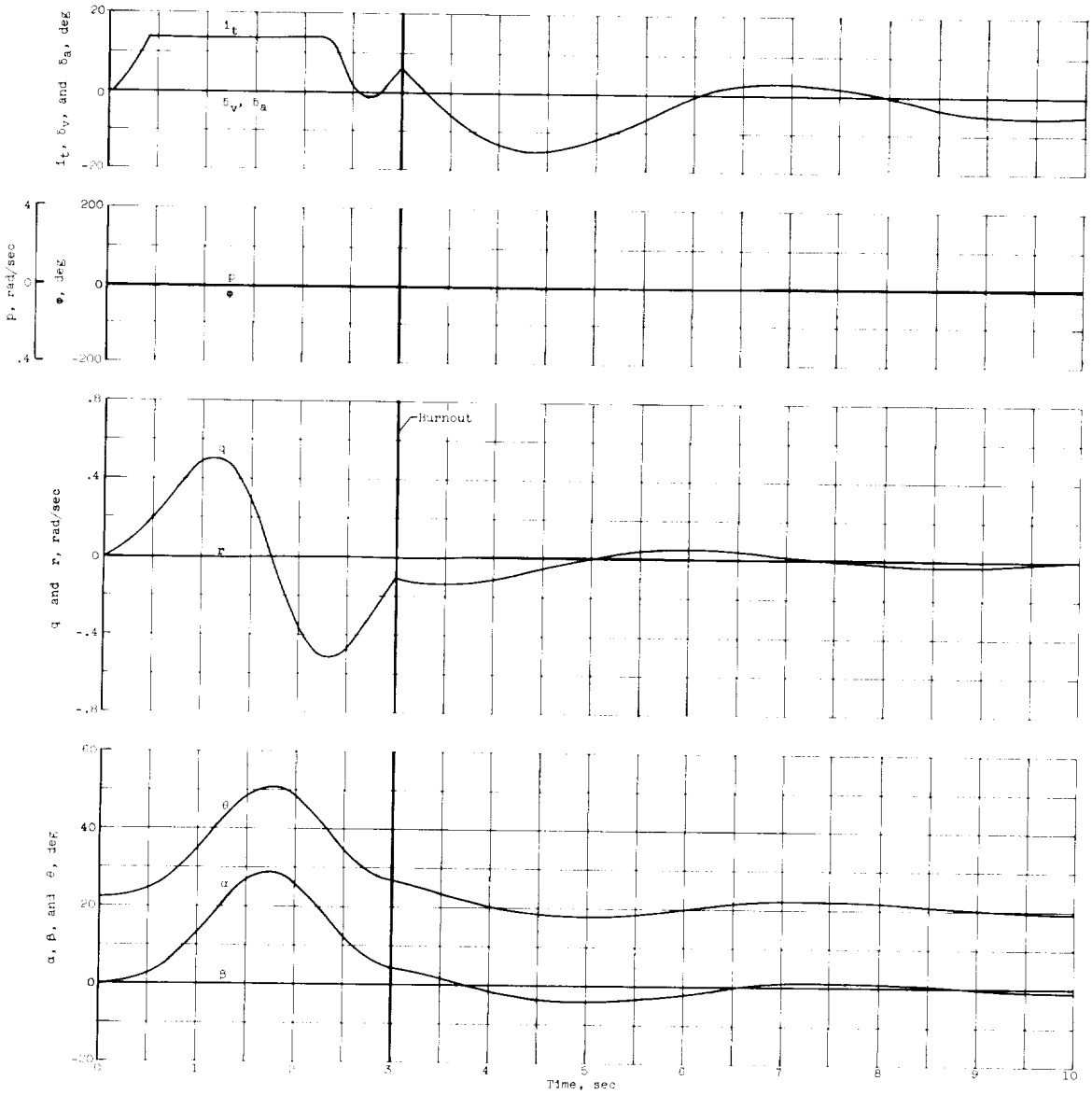

(c) Instantaneous control response.

Figure 6. - Concluded. Jet plume effect (P_2/P_1 = 17.7) on the motions with the initial conditions: $\alpha(0) = \beta(0) = p(0) = q(0) = r(0) = 0$.

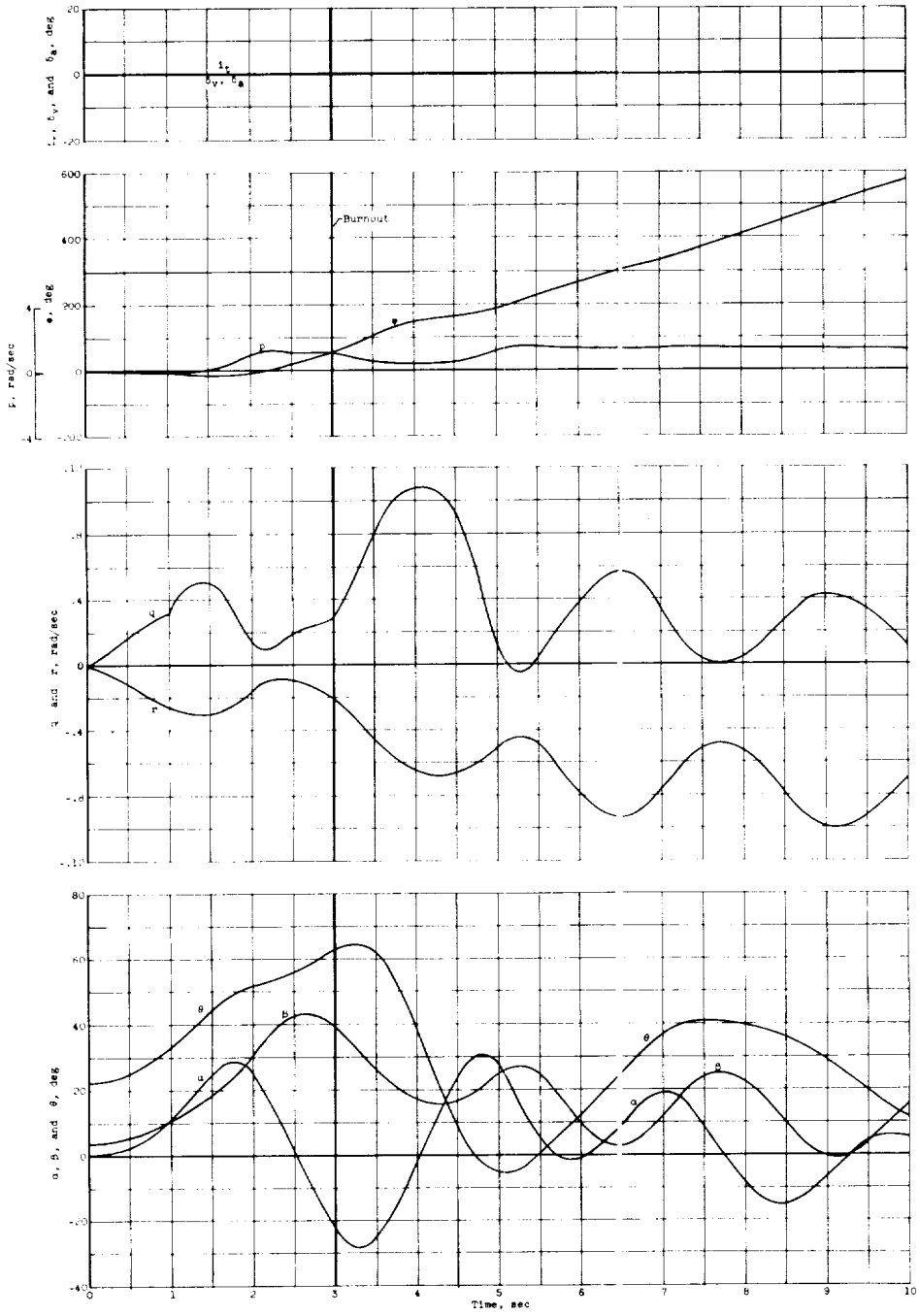

(a) Stick-fixed response.

Figure 7. - Jet plume effect (P_2/P_1 = 17.7) on the motions with the initial condition: $\beta(0) = 4^{\circ}$.

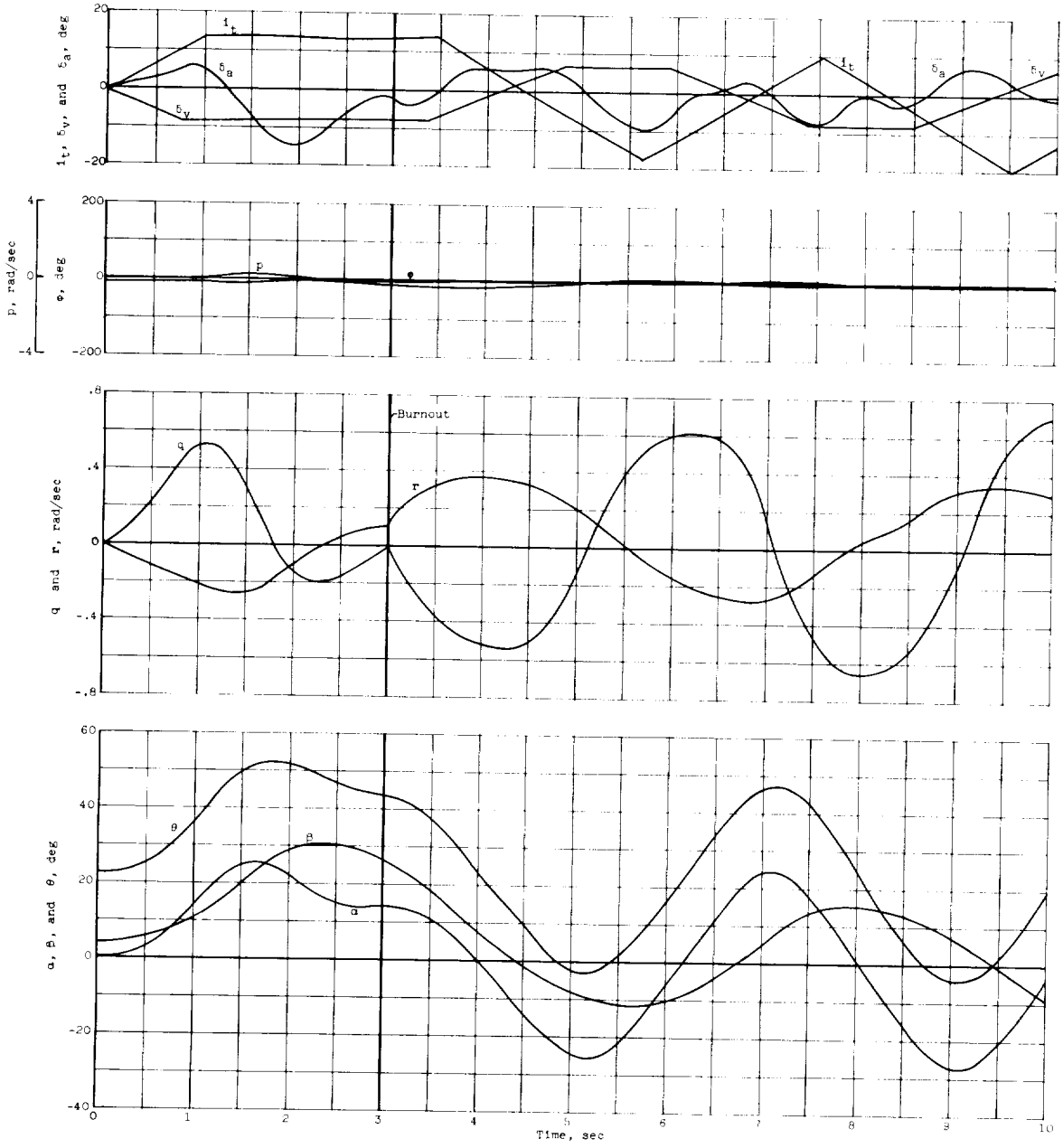

(b) Rate-limited control response.

Figure 7. - Continued. Jet plume effect (P_2/P_1 = 17.7) on the motions with initial condition: $\beta(0) = 4^\circ$.

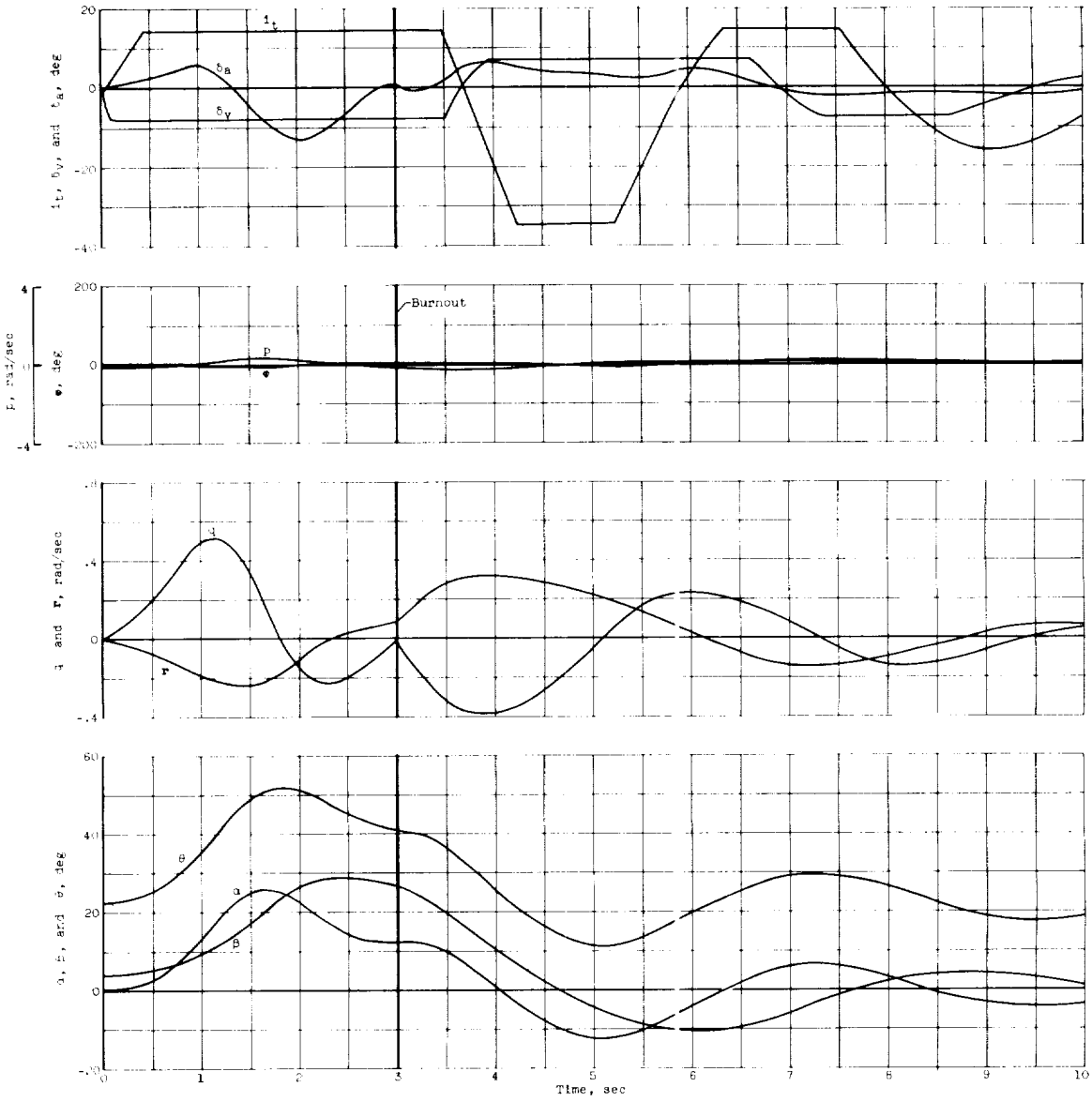

(c) Instantaneous control response.

Figure 7. - Concluded. Jet plume effect (P_2/I_1 = 17.7) on the motions with the initial condition: $\beta(0) = 4^{\circ}$.

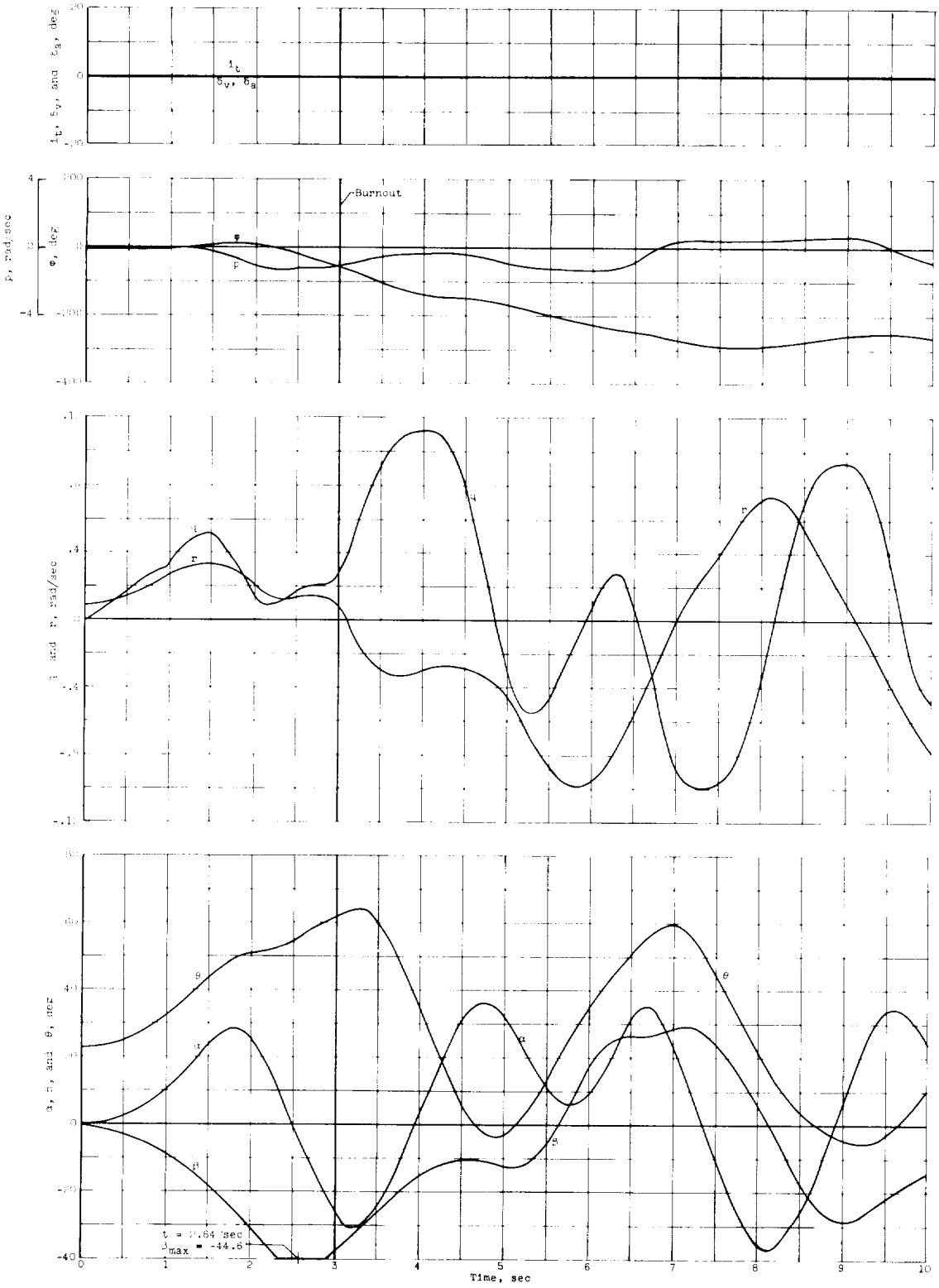

(a) Stick-fixed response.

Figure 8. - Jet plume effect (P_2/P_1 = 17.7) on the motions with the initial condition: r(0) = 0.1.

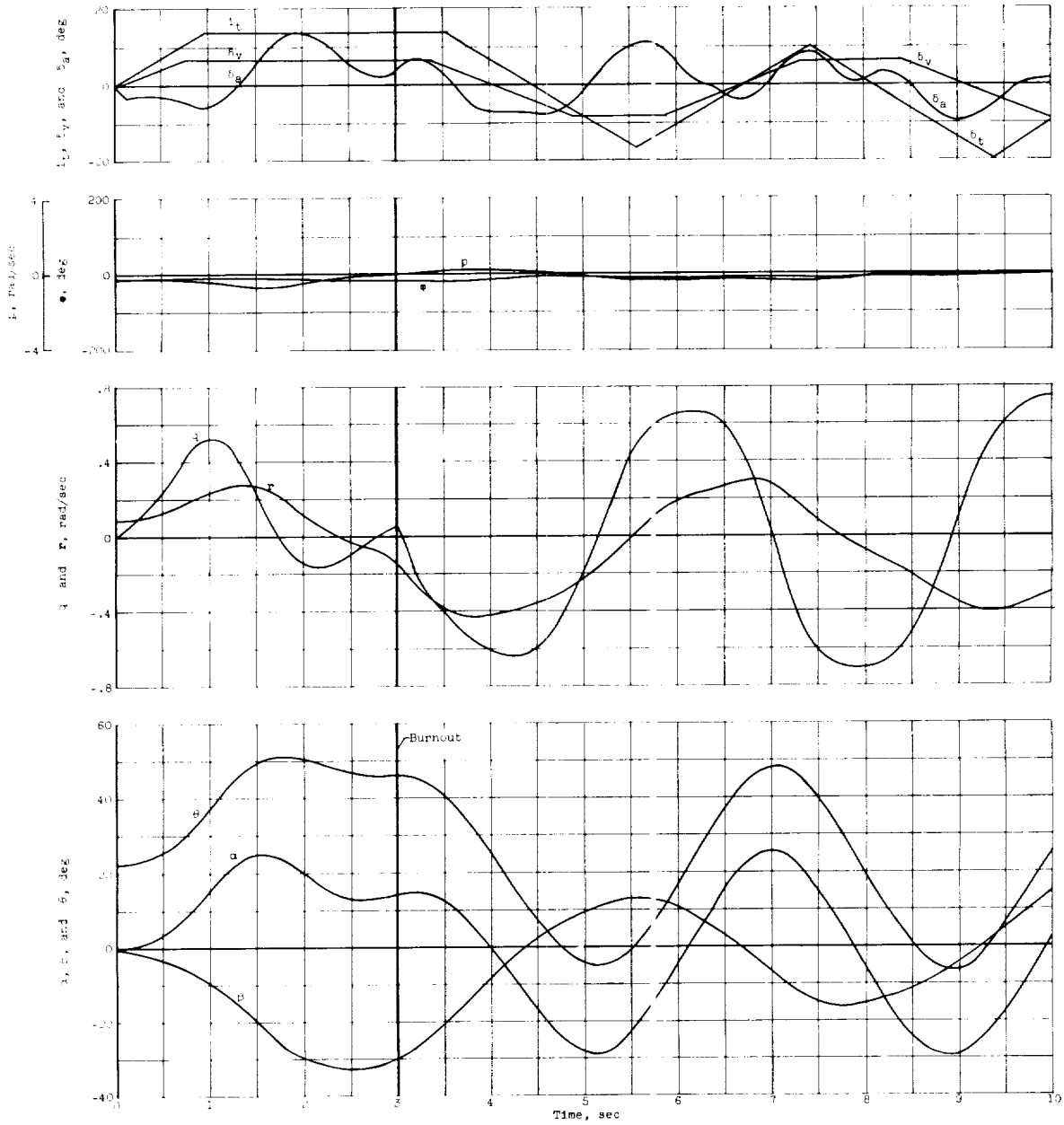

(b) Rate-limited control response.

Figure 8. - Continued. Jet plume effect (P_2/P_1 = 17.7) on the motions with the initial condition: r(0) = 0.1.

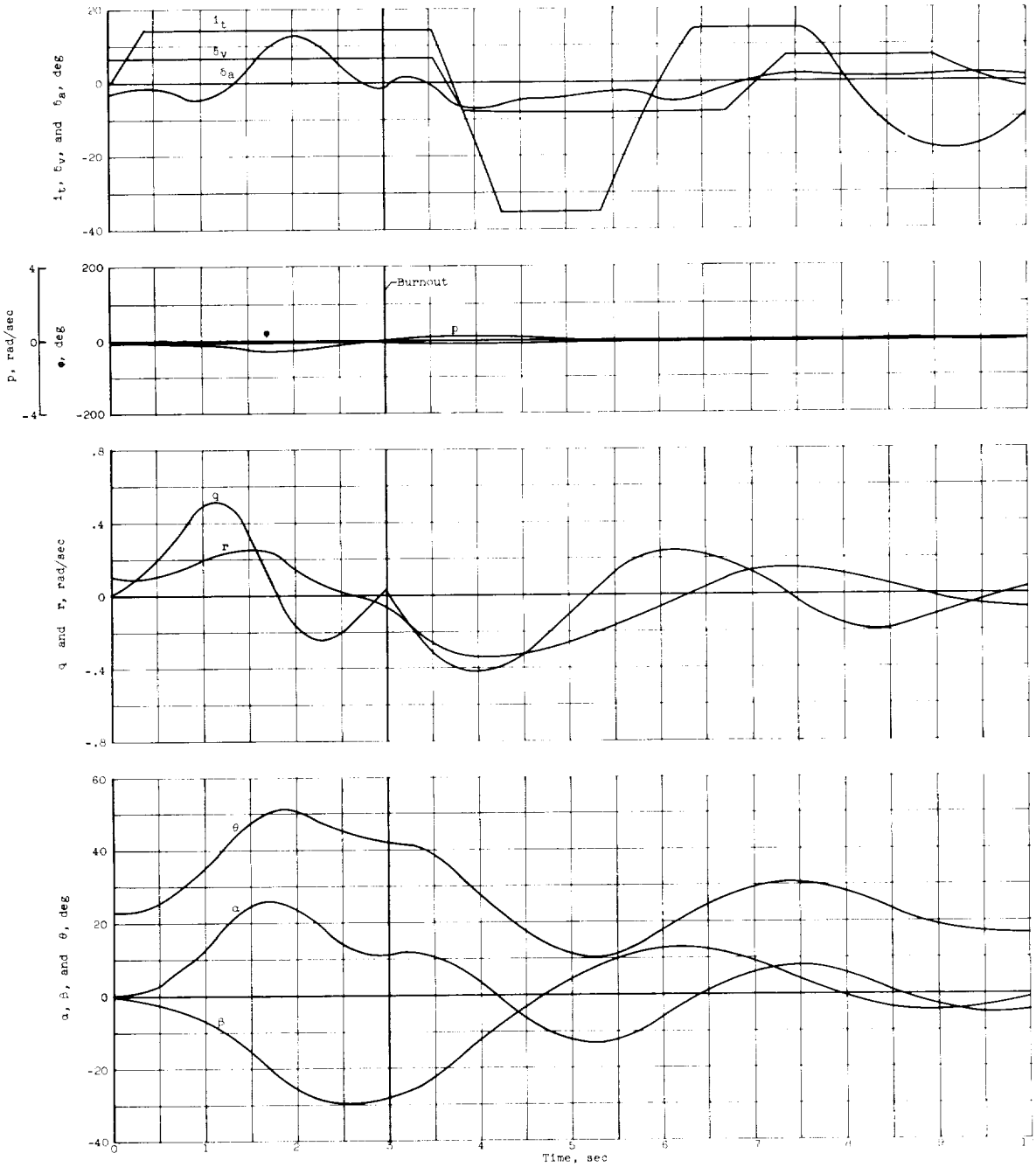

(c) Instantaneous control response.

Figure 8. - Concluded. Jet plume effect (P_2/P_1 = 17.7) on the motions with the initial condition: r(0) = 0.1.